

Accelerated Multiple Wasserstein Gradient Flows for Multi-objective Distributional Optimization

Dai Hai Nguyen¹ Dung Duc Nguyen² Atsuyoshi Nakamura¹ Hiroshi Mamitsuka³

Abstract

We study multi-objective optimization over probability distributions in Wasserstein space. Recently, Nguyen et al. (2025) introduced Multiple Wasserstein Gradient Descent (MWGraD) algorithm, which exploits the geometric structure of Wasserstein space to jointly optimize multiple objectives. Building on this approach, we propose an accelerated variant, A-MWGraD, inspired by Nesterov’s acceleration. We analyze the continuous-time dynamics and establish convergence to weakly Pareto optimal points in probability space. Our theoretical results show that A-MWGraD achieves a convergence rate of $\mathcal{O}(1/t^2)$ for geodesically convex objectives and $\mathcal{O}(e^{-\sqrt{\beta}t})$ for β -strongly geodesically convex objectives, improving upon the $\mathcal{O}(1/t)$ rate of MWGraD in the geodesically convex setting. We further introduce a practical kernel-based discretization for A-MWGraD and demonstrate through numerical experiments that it consistently outperforms MWGraD in convergence speed and sampling efficiency on multi-target sampling tasks.

1. Introduction

We study multi-objective optimization over the space of probability distributions. Let $F_1, F_2, \dots, F_K : \mathcal{P}_2(\mathcal{X}) \rightarrow \mathbb{R}$ be a set of K objective functionals ($K \geq 2$) defined on the space $\mathcal{P}_2(\mathcal{X})$ of probability distributions on $\mathcal{X} \subseteq \mathbb{R}^d$ with finite second-order moment. Our goal is to find an optimal distribution $\rho \in \mathcal{P}_2(\mathcal{X})$ that minimizes the vector-valued objective

$$\min_{\rho \in \mathcal{P}_2(\mathcal{X})} \mathbf{F}(\rho) = \min_{\rho \in \mathcal{P}_2(\mathcal{X})} (F_1(\rho), F_2(\rho), \dots, F_K(\rho)). \quad (1)$$

¹Graduate School of Information Science and Technology, Hokkaido University, Japan ²Institute of Information Technology, Vietnam Academy of Science and Technology, Vietnam

³Bioinformatics Center, Kyoto University, Japan. Correspondence to: Dai Hai Nguyen <hai@ist.hokudai.ac.jp or haidnguyen0909@gmail.com>.

This problem, known as *Multi-Objective Distributional Optimization* (MODO, Nguyen et al. (2025)), can be regarded as a natural extension of classical multi-objective optimization (MOO, Sawaragi et al. (1985)) from the Euclidean spaces to the probability spaces (or spaces of probability distributions). A motivating example is multi-target sampling (Liu et al., 2021; Phan et al., 2022), where the goal is to generate samples or particles that simultaneously approximate multiple unnormalized target distributions. In this setting, each objective corresponds to the Kullback–Leibler (KL) divergence between the current distribution and one of the targets. To solve MODO, Nguyen et al. (2025) recently proposed the *Multiple Wasserstein gradient descent* (MWGraD) algorithm, which constructs a flow of distributions that gradually decreases all the objectives. At each iteration, it (i) estimates the Wasserstein gradient of each objective F_k , for $k \in \{1, 2, \dots, K\}$, and (ii) aggregates them into a single Wasserstein gradient to update the particles.

In Euclidean optimization, standard gradient descent (GD) is often suboptimal, whereas momentum-based methods such as Nesterov’s accelerated gradient (NAG, Nesterov (2013)) achieve improved convergence rates. Its continuous-time counterpart, known as the *accelerated gradient flow* (Su et al., 2016), has been extensively studied, including in multi-objective settings (Attouch & Garrigos, 2015; Sonnag & Peitz, 2024). In the context of optimization over probability spaces, Taghvaei & Mehta (2019) introduced accelerated flows from an optimal control perspective, while Wang & Li (2022) developed a unified framework of accelerated gradient flows in probability spaces under different information metrics, including Fisher-Rao, Wasserstein, Kalman-Wasserstein, and Stein metrics. Both lines of work interpret acceleration through the lens of damped Hamiltonian dynamics.

Given the success of accelerated methods, a natural question arises: *Can MWGraD be similarly accelerated in the probability space settings?* In this work, we answer this question affirmatively. Our contributions are summarized as follows.

1. We construct a continuous-time flow, termed the *MWGraD flow* (Nguyen et al., 2025), to

analyze the convergence of MWGraD in the continuous-time limit. We define the merit function $\mathcal{M}(\rho) = \sup_{q \in \mathcal{P}_2(\mathcal{X})} \min_{k \in [K]} \{F_k(\rho) - F_k(q)\}$, where $[K] := \{1, 2, \dots, K\}$, which has been used in prior analyses of multi-objective gradient flows in Euclidean spaces (Attouch & Garrigos, 2015; Sonnag & Peitz, 2024). In Theorem 3.4, we show that **MWGraD flow achieves a convergence rate of $\mathcal{M}(\rho_t) = \mathcal{O}(1/t)$** .

2. We design an accelerated variant, *A-MWGraD*, motivated by the perspective of damped Hamiltonian dynamics for Nesterov's acceleration, and prove in Theorem 3.5 faster convergence rates: $\mathcal{M}(\rho_t) = \mathcal{O}(1/t^2)$ for geodesically convex objectives and $\mathcal{M}(\rho_t) = \mathcal{O}(e^{-\sqrt{\beta}t})$ for β -strongly geodesically convex objectives. To the best of our knowledge, this is the **first acceleration result for multi-objective optimization in probability spaces**.
3. We develop a **sampling-efficient discrete-time implementation of the accelerated flow**, incorporating practical strategies for efficiently estimating Wasserstein gradients of objectives in multi-target sampling tasks. Experiments on synthetic and real-world datasets demonstrate that A-MWGraD consistently converges faster than MWGraD, confirming the theoretical acceleration in practice.

2. Preliminaries

We begin by reviewing standard gradient flows in Euclidean and probability spaces, and then briefly introduce MODO and relevant background.

2.1. Gradient Flows on Euclidean space \mathcal{X} and Their Acceleration

Given a differentiable function $f : \mathcal{X} \rightarrow \mathbb{R}$, the Euclidean gradient flow of f is

$$\dot{\mathbf{x}}_t = -\nabla f(\mathbf{x}_t), \quad (2)$$

where ∇f denotes the Euclidean gradient. Discretizing (2) using a standard Euler integrator yields GD algorithm:

$$\mathbf{x}_{n+1} = \mathbf{x}_n - \eta_n \nabla f(\mathbf{x}_n),$$

with step size $\eta_n > 0$. GD is known to be sub-optimal; other first-order methods achieve better convergence guarantees and practical performance (Nemirovskij & Yudin, 1983; Nesterov, 2013). A key feature of these improved methods is the incorporation of a *momentum effect*. For example, Nesterov's Accelerated Gradient (NAG) method (Nesterov, 2013) updates according to

$$\begin{aligned} \mathbf{x}_n &= \mathbf{m}_{n-1} - \eta_n \nabla f(\mathbf{m}_{n-1}), \\ \mathbf{m}_n &= \mathbf{x}_n + \alpha_n (\mathbf{x}_n - \mathbf{x}_{n-1}), \end{aligned}$$

where $\alpha_n > 0$ depends on the convexity of f . For L -smooth and β -strongly convex f , $\alpha_n = (\sqrt{L} - \sqrt{\beta})/(\sqrt{L} + \sqrt{\beta})$; otherwise, $\alpha_n = (n-1)/(n+2)$. The continuous-time limit of NAG satisfies an ordinary differential equation (ODE), known as the *accelerated gradient flow* (AGF) (Su et al., 2016; Shi et al., 2022):

$$\ddot{\mathbf{x}}_t + \alpha_t \dot{\mathbf{x}}_t + \nabla f(\mathbf{x}_t) = 0, \quad (3)$$

where $\alpha_t = 2\sqrt{\beta}$ for β -strongly convex f and $\alpha_t = 3/t$ for general convex f . Importantly, AGF (3) can be formulated as a damped Hamiltonian flow (Maddison et al., 2018):

$$\begin{aligned} \dot{\mathbf{x}}_t &= \nabla_m H(\mathbf{x}_t, \mathbf{m}_t), \\ \dot{\mathbf{m}}_t &= -\alpha_t \mathbf{m}_t - \nabla_{\mathbf{x}} H(\mathbf{x}_t, \mathbf{m}_t), \end{aligned}$$

where \mathbf{x} and \mathbf{m} are the state and momentum variables, respectively, and $H(\mathbf{x}, \mathbf{m}) = f(\mathbf{x}) + \frac{1}{2}\|\mathbf{m}\|^2$ is the Hamiltonian. Thus, AGF can be interpreted as introducing a linear momentum term into the Hamiltonian dynamics.

2.2. Gradient Flows on Probability Spaces $\mathcal{P}_2(\mathcal{X})$ and Their Acceleration

Optimization over the probability space $\mathcal{P}_2(\mathcal{X})$ follows a similar principle. Given a functional $F : \mathcal{P}_2(\mathcal{X}) \rightarrow \mathbb{R}$, we require an analogue of the Euclidean gradient. The resulting gradient flow depends on the choice of metric on $\mathcal{P}_2(\mathcal{X})$.

Definition 2.1 (Metric Tensor). Let $\rho \in \mathcal{P}_2(\mathcal{X})$. The tangent space at ρ is $\mathcal{T}_\rho \mathcal{P}_2(\mathcal{X}) = \{\sigma \in \mathcal{F}(\mathcal{X}) : \int \sigma d\mathbf{x} = 0\}$, where $\mathcal{F}(\mathcal{X})$ denotes the space of smooth functions on \mathcal{X} . The cotangent space at ρ , $\mathcal{T}_\rho^* \mathcal{P}_2(\mathcal{X})$, is identified with the quotient space $\mathcal{F}(\mathcal{X})/\mathbb{R}$.

A metric tensor $G(\rho) : \mathcal{T}_\rho \mathcal{P}_2(\mathcal{X}) \rightarrow \mathcal{T}_\rho^* \mathcal{P}_2(\mathcal{X})$ is an invertible mapping defining an inner product on $\mathcal{T}_\rho \mathcal{P}_2(\mathcal{X})$:

$$g_\rho(\sigma_1, \sigma_2) = \int \sigma_1 G(\rho) \sigma_2 d\mathbf{x} = \int \Phi_1 G(\rho)^{-1} \Phi_2 d\mathbf{x},$$

where $\sigma_1, \sigma_2 \in \mathcal{T}_\rho \mathcal{P}_2(\mathcal{X})$ and $\Phi_i \in \mathcal{T}_\rho^* \mathcal{P}_2(\mathcal{X})$ is the function satisfying $\sigma_i = G(\rho)^{-1} \Phi_i$, for $i = 1, 2$.

Definition 2.2 (Gradient Flow in Probability Spaces). The gradient flow of $F(\rho)$ under metric $G(\rho)$ is

$$\dot{\rho}_t = -G(\rho_t)^{-1} \delta_\rho F[\rho_t],$$

where $\delta_\rho F[\rho] : \mathcal{X} \rightarrow \mathbb{R}$ is the first variation of F , satisfying

$$F(\rho + \epsilon \sigma) = F(\rho) + \epsilon \int \delta_\rho F[\rho](\mathbf{x}) \sigma(\mathbf{x}) d\mathbf{x},$$

for all $\sigma : \mathcal{X} \rightarrow \mathbb{R}$ with $\int \sigma(\mathbf{x}) d\mathbf{x} = 0$.

We focus on the Wasserstein-2 metric \mathcal{W}_2 , widely used in practice (Nguyen & Tsuda, 2023; Nguyen et al., 2023;

Nguyen & Sakurai, 2023; 2024). The inverse Wasserstein metric tensor is given by

$$G^W(\rho)^{-1}\Phi = -\nabla \cdot (\rho \nabla \Phi),$$

where $\nabla \cdot$ denotes the divergence operator, and the metric is

$$\begin{aligned} g_\rho^W(\sigma_1, \sigma_2) &= \int \sigma_1 G^W(\rho) \sigma_2 d\mathbf{x} \\ &= \int \Phi_1 G^W(\rho)^{-1} \Phi_2 d\mathbf{x} = \int \langle \nabla \Phi_1, \nabla \Phi_2 \rangle d\rho. \end{aligned}$$

Then, the resulting Wasserstein gradient flow is

$$\begin{aligned} \dot{\rho}_t &= -\text{grad}F(\rho_t) = -G^W(\rho_t)^{-1} \delta_\rho F[\rho_t] \\ &= \nabla \cdot (\rho_t \nabla \delta_\rho F[\rho_t]), \end{aligned}$$

where $\text{grad}F(\rho) \in T_\rho \mathcal{P}_2(\mathcal{X})$ is the Wasserstein gradient of F at ρ . See Wang & Li (2022); Nguyen & Sakurai (2023; 2024) for further details.

Hamiltonian Flows in Probability Spaces. Analogous to the Euclidean case, we can define the Hamiltonian

$$H(\rho, \Phi) = F(\rho) + \frac{1}{2} \int \Phi G(\rho)^{-1} \Phi d\mathbf{x},$$

where ρ and Φ act as the state and momentum variables, respectively. Following the damped Hamiltonian interpretation of Nesterov's acceleration (Taghvaei & Mehta, 2019; Wang & Li, 2022), the Accelerated Information Gradient (AIG) flow is given by

$$\begin{aligned} \dot{\rho}_t &= \delta_\Phi H(p_t, \Phi_t), \\ \dot{\Phi}_t + \alpha_t \Phi_t + \delta_\rho H(p_t, \Phi_t) &= 0. \end{aligned}$$

Under the Wasserstein-2 metric, this reduces to the Wasserstein accelerated gradient flow (W-AIG, Wang & Li (2022)) :

$$\begin{aligned} \dot{\rho}_t + \nabla \cdot (\rho_t \nabla \Phi_t) &= 0, \\ \dot{\Phi}_t + \alpha_t \Phi_t + \frac{1}{2} \|\Phi_t\|^2 + \delta_\rho H(p_t, \Phi_t) &= 0. \end{aligned} \tag{4}$$

2.3. Multiple Wasserstein Gradient Descent Algorithm for MODO

The goal of MODO (1) is to optimize multiple objectives over probability space simultaneously. As in classical MOO, different distributions may perform better on different objectives, which motivates the notion of Pareto optimality.

Definition 2.3. Consider the optimization problem (1).

1. A distribution $p^* \in \mathcal{P}_2(\mathcal{X})$ is Pareto optimal if there does not exist another $q \in \mathcal{P}_2(\mathcal{X})$ such that $F_k(q) \leq F_k(p^*)$ for all $k \in [K]$ and $F_l(q) < F_l(p^*)$ for at least one index $l \in [K]$. We denote the set of all Pareto optimal distributions by P^* .

2. A distribution $p^* \in \mathcal{P}_2(\mathcal{X})$ is weakly Pareto optimal if there does not exist another $q \in \mathcal{P}_2(\mathcal{X})$ such that $F_k(q) < F_k(p^*)$ for all $k \in [K]$. We denote the set of all weakly Pareto optimal distributions by P_w^* .

From Definition 2.3, it follows that $P^* \subset P_w^*$. However, the definition cannot directly be used in practice to check whether a distribution is Pareto optimal. Nguyen et al. (2025) introduced the definition of *Pareto stationary distribution*, which extends the definition of Pareto stationary points in Euclidean space, as follows.

Definition 2.4. We denote the probability simplex as Let $\mathcal{W} = \left\{ \mathbf{w} = (w_1, \dots, w_K)^\top \mid \mathbf{w} \geq 0, \sum_{k=1}^K w_k = 1 \right\}$.

A distribution $\rho \in \mathcal{P}_2(\mathcal{X})$ is Pareto stationary or critical if

$$\min_{\mathbf{w} \in \mathcal{W}} \langle \text{grad}F(\rho)\mathbf{w}, \text{grad}F(\rho)\mathbf{w} \rangle_\rho = 0,$$

where

$\text{grad}F(\rho)(\mathbf{x}) = [\text{grad}F_1(\rho)(\mathbf{x}), \dots, \text{grad}F_K(\rho)(\mathbf{x})]$, and $\text{grad}F(\rho)(\mathbf{x})\mathbf{w} = \sum_{k=1}^K w_k \text{grad}F_k(\rho)(\mathbf{x})$. We denote the set of all Pareto stationary distributions by P_c^* .

It can be verified that, in the geodesically convex setting, the stationarity conditions are also sufficient conditions for weak Pareto optimality, and we have that $P^* \subset P_w^* = P_c^*$.

MWGrAD (Nguyen et al., 2025) is designed to find a Pareto stationary distribution by iteratively constructing distributions $\rho_0, \rho_1, \dots, \rho_T$, starting from a simple initial distribution ρ_0 (e.g., a standard Gaussian), and simultaneously decreasing all objectives. At iteration n , MWGrAD seeks a tangent direction s_n that maximizes the minimum decrease across objectives:

$$\begin{aligned} &\max_{s \in T_{\rho_n} \mathcal{P}_2(\mathcal{X})} \min_{k \in [K]} \frac{1}{h} (F_k(\rho_n) - F_k(\gamma(h))) \\ &\approx \max_{\mathbf{v} \in \mathcal{V}} \min_{k \in [K]} \int \langle \nabla \delta F_k(\rho_n), \mathbf{v} \rangle d\rho_n, \end{aligned} \tag{5}$$

where $\mathbf{v} : \mathcal{X} \rightarrow \mathcal{X}$ is a vector field belonging to the space of vector fields \mathcal{V} ; s and \mathbf{v} are related through the elliptic equation $s = \nabla \cdot (q_n \mathbf{v})$. Here, $\gamma : [0, 1] \rightarrow \mathcal{P}_2(\mathcal{X})$ is a curve satisfying that $\gamma(0) = \rho_n$ and $\gamma'(0) = s$. To regularize the update direction (i.e., vector field \mathbf{v}), a regularization term is introduced to (5) and we can solve for s_n by optimizing

$$\max_{\mathbf{v} \in \mathcal{V}} \min_{k \in [K]} \int_{\mathcal{X}} \langle \nabla \delta_\rho F_k(\rho_n), \mathbf{v} \rangle d\rho_n - \frac{1}{2} \int_{\mathcal{X}} \|\mathbf{v}\|_2^2 d\rho_n. \tag{6}$$

The optimal \mathbf{v}_n to (6) is

$$\mathbf{v}_n = \sum_{k=1}^K w_k^{(n)} \nabla \delta_\rho F_k[\rho_n], \tag{7}$$

where

$$\mathbf{w}^{(n)} = \arg \min_{\mathbf{w} \in \mathcal{W}} \frac{1}{2} \int \left\| \sum_{k=1}^K w_k \nabla \delta_p F_k(\rho_n) \right\|_2^2 d\rho_n. \quad (8)$$

The optimal \mathbf{v}_n is used to update the current particles from $\mathbf{x}_n \sim \rho_n$ to $\mathbf{x}_{n+1} \sim \rho_{n+1}$ via $\mathbf{x}_{n+1} = \mathbf{x}_n - \eta_n \mathbf{v}_n$.

3. Multiple Wasserstein Gradient Flow and Its Acceleration

In this section, we characterize the convergence rate of MWGraD in the continuous-time limit. The velocity field \mathbf{v}_n (7) specifies how particles $\mathbf{x}_n \sim \rho_n$ are transported to $\mathbf{x}_{n+1} \sim \rho_{n+1}$. Taking the limit $\eta_n \rightarrow 0$, the MWGraD updates converge to the following probability flow, which we term the *MWGraD flow*:

$$\begin{aligned} \dot{\rho}_t + \nabla \cdot (\rho_t \nabla \Phi_t) &= 0, \\ \Phi_t + \text{proj}_{\mathcal{C}(\rho_t), \rho_t}[0] &= 0, \end{aligned} \quad (9)$$

where $\mathcal{C}(\rho) = \text{conv}(\{\delta_p F_k[\rho] : k = 1, 2, \dots, K\})$ denotes the convex hull of the first variations of objectives F_k ($k \in [K]$). Here, $\text{proj}_{\mathcal{K}, \rho}[f]$ denotes the projection of a function $f \in T_\rho^* \mathcal{P}(\mathcal{X})$ onto a closed convex set $\mathcal{K} \subset T_\rho^* \mathcal{P}(\mathcal{X})$ under the Wasserstein-2 metric:

$$\begin{aligned} \text{proj}_{\mathcal{K}, \rho}[f] &= \arg \min_{h \in \mathcal{K}} \int (f - h) G^W(\rho)^{-1} (f - h) d\mathbf{x} \\ &= \arg \min_{h \in \mathcal{K}} \int \|\nabla f - \nabla h\|^2 d\rho. \end{aligned} \quad (10)$$

This formulation makes explicit how MWGraD can be interpreted as a continuous-time gradient flow over probability distributions, where the convex combinations of Wasserstein gradients enforce a Pareto-stationary descent direction.

3.1. Convergence Analysis of MWGraD flow

To analyze the convergence rate of the MWGraD flow (9) for MODO (1), we introduce the following *merit function*:

$$\mathcal{M}(\rho) = \sup_{q \in \mathcal{P}(\mathcal{X})} \min_{k \in [K]} \{F_k(\rho) - F_k(q)\}. \quad (11)$$

This definition naturally generalizes the merit function used to analyze convergence of function values for MOO in Euclidean spaces (Sonntag & Peitz, 2024; Tanabe et al., 2023). Importantly, for all $\rho \in \mathcal{P}_2(\mathcal{X})$, we have $\mathcal{M}(\rho) \geq 0$, and ρ is weakly Pareto optimal if and only if $\mathcal{M}(\rho) = 0$. This follows directly from the argument in Theorem 3.1 of (Tanabe et al., 2023).

We establish the convergence rate of the MWGraD flow (9) by showing that $\mathcal{M}(\rho_t)$ converges to zero under the following assumption.

Assumption 3.1. For $\mathbf{u} \in \mathbb{R}^K$, define the level set: $\Omega_{\mathbf{F}}(\mathbf{u}) = \{q \in \mathcal{P}(\mathcal{X}) | \mathbf{F}(q) \leq \mathbf{u}\}$. Assume that for any $q \in \mathcal{P}_2(\mathcal{X})$, there exists $p^* \in P_w^*$ such that $\mathbf{F}(p^*) \leq \mathbf{F}(q)$, and that

$$R = \sup_{\mathbf{F}^* \in \mathbf{F}(P_w^* \cap \Omega_{\mathbf{F}}(\mathbf{F}(\rho_0)))} \inf_{q \in \mathbf{F}^{-1}(\{\mathbf{F}^*\})} \mathcal{W}_2^2(q, \rho_0) < \infty.$$

Remarks.

- Assumption 3.1 is extended from Assumption 5.2 in (Tanabe et al., 2023) from the Euclidean space to probability space.
- In the single-objective cases ($K = 1$), Assumption 3.1 holds if the optimization problem has at least one optimal solution. Indeed, for $K = 1$, P_w^* coincides with the set of optimal solutions, $P_w^* \cap \Omega_{\mathbf{F}}(\mathbf{F}(p_0)) = P_w^*$, and $R = \inf_{p^* \in P_w^*} \mathcal{W}_2^2(p^*, p_0) < \infty$.

To facilitate the convergence analysis, we next introduce an auxiliary lemma that allows evaluating the merit function (11) without taking the supremum over the entire space $\mathcal{P}_2(\mathcal{X})$.

Lemma 3.2. Let $\rho_0 \in \mathcal{P}_2(\mathcal{X})$ and $\rho \in \Omega_{\mathbf{F}}(\mathbf{F}(\rho_0))$. Define

$$E_k(\rho, q) = F_k(\rho) - F_k(q), E(\rho, q) = \min_{k \in [K]} E_k(\rho, q).$$

Then

$$\sup_{\mathbf{F}^* \in \mathbf{F}(P_w^* \cap \Omega_{\mathbf{F}}(\mathbf{F}(\rho_0)))} \inf_{q \in \mathbf{F}^{-1}(\{\mathbf{F}^*\})} E(\rho, q) = \sup_{q \in \mathcal{P}_2(\mathcal{X})} E(\rho, q).$$

The proof is deferred to Appendix A. We further impose the following assumption on the objectives F_k (for $k \in [K]$).

Assumption 3.3 (β -strongly geodesic convexity). Each objective F_k is β -strongly geodesically convex with respect to the Wasserstein-2 distance, for $k \in [K]$, in the sense that for $\forall p, q \in \mathcal{P}_2(\mathcal{X})$

$$\begin{aligned} F_k(q) &\geq F_k(p) + \langle \text{grad} F_k(p), \text{Exp}_p^{-1}(q) \rangle_p + \frac{\beta}{2} \mathcal{W}_2^2(p, q) \\ &= F_k(p) + \int \langle \nabla \delta_p F_k(p)(\mathbf{x}), T(\mathbf{x}) - \mathbf{x} \rangle d\mathbf{x} \\ &\quad + \frac{\beta}{2} \int \|\mathbf{x} - T(\mathbf{x})\|^2 d\mathbf{x}, \end{aligned}$$

where Exp_p denotes the exponential mapping, which specifies how to move p along a tangent vector on $\mathcal{P}_2(\mathcal{X})$, Exp_p^{-1} denotes its inversion mapping, which maps a point on $\mathcal{P}_2(\mathcal{X})$ to a tangent vector, T is the optimal transport mapping from p to q . If $\beta = 0$, F_k is said to be geodesically convex with respect to the Wasserstein-2 distance. We refer to (Santambrogio, 2015) for details.

We are now ready to state the convergence result for the MWGraD flow (9).

Theorem 3.4. *Let ρ_t be the solution of the MWGraD flow (9). Suppose that each F_k is geodesically convex for $k \in [K]$, and that Assumption 3.1 holds. Then for all $t \geq 0$,*

$$\mathcal{M}(\rho_t) \leq \frac{R}{2t} = \mathcal{O}\left(\frac{1}{t}\right).$$

Sketch of Proof. (See Appendix B for details) For any $q \in \mathcal{P}_2(\mathcal{X})$, define the Lyapunov functional

$$\mathcal{V}(q, t) = \frac{1}{2} \mathcal{W}_2^2(\rho_t, q) = \frac{1}{2} \int \|T_t(\mathbf{x}) - \mathbf{x}\|^2 d\rho_t(\mathbf{x}),$$

where T_t is the optimal transport map from ρ_t to q . We can show that $E_k(\rho_t, q)$ and $E(\rho_t, q)$ are non-increasing in time, i.e., $\dot{E}_k(\rho_t, q) \leq 0$ and $\dot{E}(\rho_t, q) \leq 0$ for all k . Moreover,

$$E(\rho_t, q) \leq -\dot{\mathcal{V}}(q, t). \quad (12)$$

Integrating (12) over $[0, t]$ gives

$$E(\rho_t, q) \leq \frac{\mathcal{V}(q, 0)}{t} = \frac{\mathcal{W}_2^2(\rho_0, q)}{2t}.$$

By Assumption 3.1,

$$\sup_{\mathbf{F}^* \in \mathbf{F}(P^* \cap \Omega_{\mathbf{F}}(\mathbf{F}(\rho_0)))} \inf_{q \in \mathbf{F}^{-1}(\{\mathbf{F}^*\})} E(\rho_t, q) \leq \frac{R}{2t}.$$

Since $E_k(\rho_t, q)$ is non-increasing, it follows that $F_k(\rho_t) - F_k(q) \leq F_k(\rho_0) - F_k(q)$ for $k \in [K]$, which means that $\rho_t \in \Omega_{\mathbf{F}}(\mathbf{F}(\rho_0))$. Applying Lemma 3.2 completes the proof.

3.2. Accelerated MWGraD Flow and Its Convergence Analysis

Inspired by AIG flow (Taghvaei & Mehta, 2019; Wang & Li, 2022), we introduce the *accelerated MWGraD flow* (A-MWGraD) as follows:

$$\begin{aligned} \dot{\rho}_t + \nabla \cdot (\rho_t \nabla \Phi_t) &= 0, \\ \dot{\Phi}_t + \alpha_t \Phi_t + \frac{1}{2} \|\nabla \Phi_t\|^2 + \text{proj}_{\mathcal{C}(\rho_t), \rho_t}[0] &= 0. \end{aligned} \quad (13)$$

It can be verified that when $K = 1$, (13) reduces to the W-AIG (4). We now characterize the convergence rate of the A-MWGraD flow by showing that the merit function $\mathcal{M}(\rho_t)$ converges to 0 at an accelerated rate of $\mathcal{O}(1/t^2)$ for geodesically convex objectives and $\mathcal{O}(e^{-\sqrt{\beta}t})$ for β -strongly geodesically convex objectives.

Theorem 3.5. *Let ρ_t be the solution of the A-MWGraD flow (13). Suppose that each F_k is geodesically convex for*

$k \in [K]$, and let $\alpha_t = \alpha/t$ with $\alpha \geq 3$. Under Assumption 3.1,

$$\mathcal{M}(\rho_t) \leq \frac{(\alpha - 1)R}{t^2} = \mathcal{O}\left(\frac{1}{t^2}\right), \text{ for all } t \geq 0. \quad (14)$$

Suppose that each F_k is β -strongly geodesically convex for $k \in [K]$ with $\beta > 0$, and let $\alpha_t = 2\sqrt{\beta}$. Under Assumption 3.1,

$$\begin{aligned} \mathcal{M}(\rho_t) &\leq e^{-\sqrt{\beta}t} \left[\min_{l \in [K]} F_l(\rho_0) + \frac{\beta R}{2} \right] = \mathcal{O}(e^{-\sqrt{\beta}t}), \\ &\text{for all } t \geq 0. \end{aligned} \quad (15)$$

Sketch of Proof of (14). (See Appendix C for the detailed proofs of (14) and (15)) For each $k \in [K]$, define the Lyapunov functional

$$\begin{aligned} \mathcal{E}_{k,\lambda}(\rho_t, q) &= t^2(F_k(\rho_t) - F_k(q)) \\ &+ \frac{1}{2} \int \|2(\mathbf{x} - T_t(\mathbf{x})) + t\nabla\Phi_t(\mathbf{x})\|^2 d\rho_t(\mathbf{x}) \\ &+ \frac{\lambda}{2} \int \|\mathbf{x} - T_t(\mathbf{x})\|^2 d\rho_t(\mathbf{x}), \end{aligned}$$

and let

$$\mathcal{E}_\lambda(\rho_t, q) = \min_{k \in [K]} \mathcal{E}_{k,\lambda}(\rho_t, q).$$

With the choice $\lambda = 2(\alpha - 3)$, it can be shown that $\mathcal{E}_\lambda(\rho_t, q)$ is non-increasing in time, i.e. $\dot{\mathcal{E}}_\lambda(\rho_t, q) \leq 0$. Consequently,

$$\begin{aligned} E(\rho_t, q) &= \min_{k \in [K]} \{F_k(\rho_t) - F_k(q)\} \leq \frac{\mathcal{E}_\lambda(\rho_t, q)}{t^2} \\ &\leq \frac{\mathcal{E}_\lambda(\rho_0, q)}{t^2} = \frac{(\alpha - 1)\mathcal{W}_2^2(\rho_0, q)}{t^2}. \end{aligned}$$

By Assumption 3.1, this yields

$$\sup_{\mathbf{F}^* \in \mathbf{F}(P_w^* \cap \Omega_{\mathbf{F}}(\mathbf{F}(\rho_0)))} \inf_{q \in \mathbf{F}^{-1}(\{\mathbf{F}^*\})} E(\rho_t, q) \leq \frac{(\alpha - 1)R}{t^2}.$$

Moreover, by Corollary C.2, $F_k(\rho_t) \leq F_k(\rho_0)$ for all k , which ensures that $\rho_t \in \Omega_{\mathbf{F}}(\mathbf{F}(\rho_0))$. Applying Lemma 3.2 completes the proof of (14).

3.3. Particle Implementation of A-MWGraD Flow

To design fast sampling algorithms, we reformulate the evolution of probability distributions in terms of particle dynamics. Suppose that $\mathbf{x}_t \sim \rho_t$ and $\mathbf{v}_t = \nabla\Phi_t(\mathbf{x}_t)$ denotes the position and the velocity of a particle at time t , respectively. Then the A-MWGraD flow (13) induces the following particle dynamics:

$$\begin{aligned} \dot{\mathbf{x}}_t &= \mathbf{v}_t, \\ \dot{\mathbf{v}}_t + \alpha_t \mathbf{v}_t + \sum_{k=1}^K w_k^{(t)} \nabla \delta_\rho F_k[\rho_t](\mathbf{x}_t) &= 0. \end{aligned} \quad (16)$$

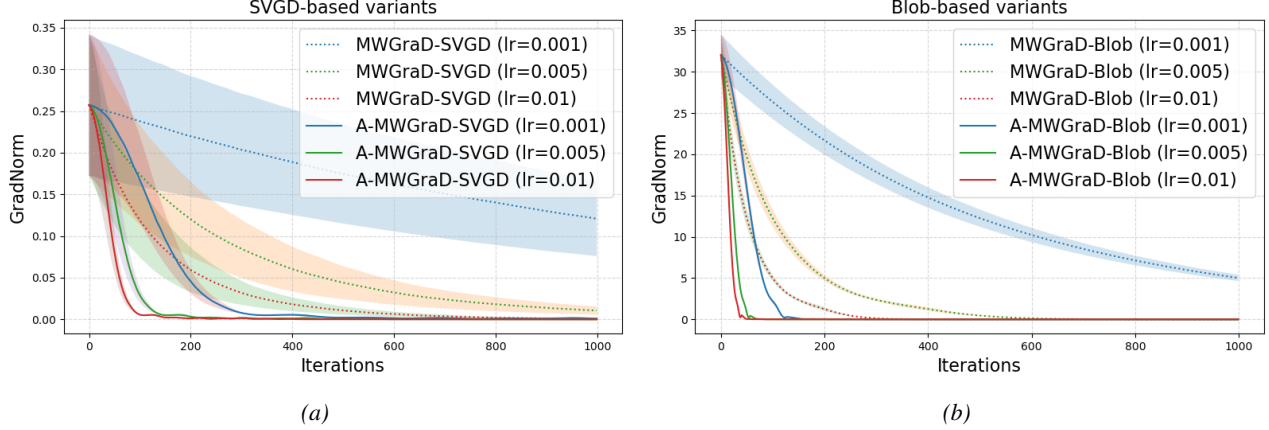


Figure 1. Convergence comparison: (a) SVGD-based variants, (b) Blob-based variants. The plot show mean and standard deviation of GradNorm over 1000 iterations with three different step sizes of $\eta = 0.001, 0.005, 0.01$.

See Appendix D for the detailed derivation.

A typical choice of $F_k(\rho)$ for sampling is the KL divergence

$$F_k(\rho) = KL(\rho || \pi_k) = \int f_k d\rho + \int \log \rho d\rho,$$

where the target distributions satisfy $\pi_k \propto \exp(-f_k)$ for $k \in [K]$. In this case, the particle dynamics become

$$\dot{\mathbf{x}}_t = \mathbf{v}_t, \dot{\mathbf{v}}_t + \alpha_t \mathbf{v}_t + \sum_{k=1}^K w_k^{(t)} \Delta_k^{(t)}(\mathbf{x}_t) = 0,$$

where $\Delta_k^{(t)} = \nabla f_k + \nabla \log \rho_t$ is the Wasserstein gradient of the KL divergence.

Discrete-Time Particle System. Consider a particle systems $\{\mathbf{x}_i^{(0)}\}_{i=1}^m$ with initial velocities $\mathbf{v}_i^{(0)} = 0$ for $i \in [m]$. At iteration n , the discretized update with step size $\eta > 0$ is given by

$$\begin{aligned} \mathbf{x}_i^{(n+1)} &= \mathbf{x}_i^{(n)} + \sqrt{\eta} \mathbf{v}_i^{(n)}, \\ \mathbf{v}_i^{(n+1)} &= \alpha_n \mathbf{v}_i^{(n)} - \sqrt{\eta} \sum_{k=1}^K w_k^{(n)} \Delta_k^{(n)}(\mathbf{x}_i^{(n)}), \end{aligned}$$

where the momentum parameter is $\alpha_n = (n-1)/(n+2)$ which corresponds to the continuous-time choice $\alpha_t = 3/t$ when the objectives are geodesically convex, or $\alpha_n = (1 - \sqrt{\beta\eta})/(1 + \sqrt{\beta\eta})$ which corresponds to the continuous-time choice $\alpha_t = 2\sqrt{\beta}$ when the objectives are β -strongly geodesically convex. However, direct computation of $\log \rho_n(\mathbf{x})$ is not feasible for empirical measures $\rho_n(\mathbf{x})$. Following (Nguyen et al., 2025), we therefore adopt kernel-based approximations, namely Stein Variational Gradient Descent (SVGD, Liu & Wang (2016)) and Blob methods (Carrillo et al., 2019).

For SVGD (Liu & Wang, 2016), we approximate $\Delta_k^{(n)}$ by $\bar{\Delta}_k^{(n)}$ (for $k \in [K]$), given by

$$\begin{aligned} \bar{\Delta}_k^{(n)}(\mathbf{x}) &= \mathbb{E}_{\mathbf{y} \sim \rho_n} [K(\mathbf{x}, \mathbf{y}) (\nabla f_k(\mathbf{y}) + \nabla \log \rho_n(\mathbf{y}))] \\ &= \int_{\mathcal{X}} K(\mathbf{x}, \mathbf{y}) \nabla f_k(\mathbf{y}) \rho_n(\mathbf{y}) d\mathbf{y} - \int_{\mathcal{X}} \nabla_{\mathbf{y}} K(\mathbf{x}, \mathbf{y}) \rho_n(\mathbf{y}) d\mathbf{y}, \end{aligned}$$

where the second equality follows from integration by parts. Consequently, the particle approximation of $\Delta_k^{(n)}$ is

$$\begin{aligned} \bar{\Delta}_k^{(n)}(\mathbf{x}_i^{(n)}) &= \sum_{j=1}^m K(\mathbf{x}_i^{(n)}, \mathbf{x}_j^{(n)}) \nabla f_k(\mathbf{x}_j^{(n)}) \\ &\quad - \sum_{j=1}^m \nabla_{\mathbf{x}_j^{(n)}} K(\mathbf{x}_i^{(n)}, \mathbf{x}_j^{(n)}). \end{aligned} \tag{17}$$

For Blob methods (Carrillo et al., 2019), we approximate $\Delta_k^{(n)}$ as follows

$$\begin{aligned} \bar{\Delta}_k^{(n)}(\mathbf{x}_i^{(n)}) &= \nabla f_k(\mathbf{x}_i^{(n)}) \\ &\quad - \sum_{j=1}^m \nabla_{\mathbf{x}_j^{(n)}} K(\mathbf{x}_i^{(n)}, \mathbf{x}_j^{(n)}) / \sum_{l=1}^m K(\mathbf{x}_j^{(n)}, \mathbf{x}_l^{(n)}) \\ &\quad - \sum_{j=1}^m \nabla_{\mathbf{x}_j^{(n)}} K(\mathbf{x}_i^{(n)}, \mathbf{x}_j^{(n)}) / \sum_{l=1}^m K(\mathbf{x}_i^{(n)}, \mathbf{x}_j^{(n)}). \end{aligned} \tag{18}$$

We refer the reader to Proposition 3.12 of (Carrillo et al., 2019) for the detailed derivation. The overall algorithms of MWGraD and A-MWGraD are summarized in Appendix E.

4. Numerical Experiments

In this section, we present numerical experiments demonstrating the acceleration effect of A-MWGraD flow (13). The code will be released upon acceptance.

4.1. Experiments on toy examples

We consider the task of sampling from multiple target distributions, where each target is a mixture of two Gaussians: $\pi_k(\mathbf{x}) = \gamma_{k1}\mathcal{N}(\mathbf{x}|\mu_{k1}, \Sigma_{k1}) + \gamma_{k2}\mathcal{N}(\mathbf{x}|\mu_{k2}, \Sigma_{k2})$, $k = 1, 2, 3, 4$, with mixture weights $\gamma_{k1} = 0.7$, $\gamma_{k2} = 0.3$ for all k . The component means are given by $\mu_{11} = [4, -4]^\top$, $\mu_{12} = [0.1, 0.2]^\top$, $\mu_{21} = [-4, 4]^\top$, $\mu_{22} = [-0.1, 0.3]^\top$, $\mu_{31} = [-4, -4]^\top$, $\mu_{32} = [0.4, -0.4]^\top$, $\mu_{41} = [4, 4]^\top$, $\mu_{42} = [-0.2, 0.3]^\top$, and all covariance matrices Σ_{kj} are set to the identity matrix of size 2×2 , for $k = 1, 2, 3, 4$ and $j = 1, 2$.

We represent ρ using 50 particles, initially sampled from a standard Gaussian. The particles are updated using MOO-SVGD (Liu et al., 2021), MWGraD variants (Nguyen et al., 2025) (MWGraD-SVGD and MWGraD-Blob), and the proposed accelerated variants (A-MWGraD-SVGD and A-MWGraD-Blob). Figure 3 in Appendix F shows the target distributions sharing a common high-density region around the origin. To approximate $\bar{\Delta}_k^{(n)}(\mathbf{x})$ (see (17) and (18)), we use a Gaussian kernel with fixed bandwidth 1. For the A-MWGraD variants, we set $\alpha_n = (n - 1)/(n + 2)$. To compare MWGraD and A-MWGraD variants, we compute the approximate squared norm of the combined Wasserstein gradients over the particles:

$$\text{GradNorm} = \frac{1}{m} \sum_{i=1}^m \left\| \sum_{k=1}^K w_k^{(n)} \bar{\Delta}_k^{(n)}(\mathbf{x}_i^{(n)}) \right\|^2. \quad (19)$$

It can be verified that (19) provides an approximation of the squared norm of the velocity $\mathbf{v}^{(n)}$ in (7). As (19) approaches zero, the distribution ρ_n approaches a Pareto stationary distribution. In this experiment, we perform five independent trials and record the values of GradNorm . Figure 1 report the mean and standard deviation of this quantity over 1000 iterations of particle updates for both the SVGD-based and Blob-based variants. We evaluate three different step sizes of $\eta = 0.001, 0.005, 0.01$. We observe that, across all step sizes, the A-MWGraD variants consistently achieve low values of GradNorm faster than their MWGraD counterparts.

Furthermore, Figure 3 in Appendix F visualizes the evolution of the 50 particles updated by different methods across iterations using a fixed step size 0.001. We see that particles by MOO-SVGD spread across all modes of the target distributions after 2000 iterations, while particles updated by MWGraD and A-MWGraD variants concentrate on the shared high-density region. Notably, the A-MWGraD variants converge significantly faster than MWGraD variants: for example, MWGraD-Blob requires approximately 500 iterations to cover the high-density region, while A-MWGraD-Blob achieves this within only 50 iterations. These results visually and quantitatively confirms the acceleration effect of A-MWGraD in this toy setting.

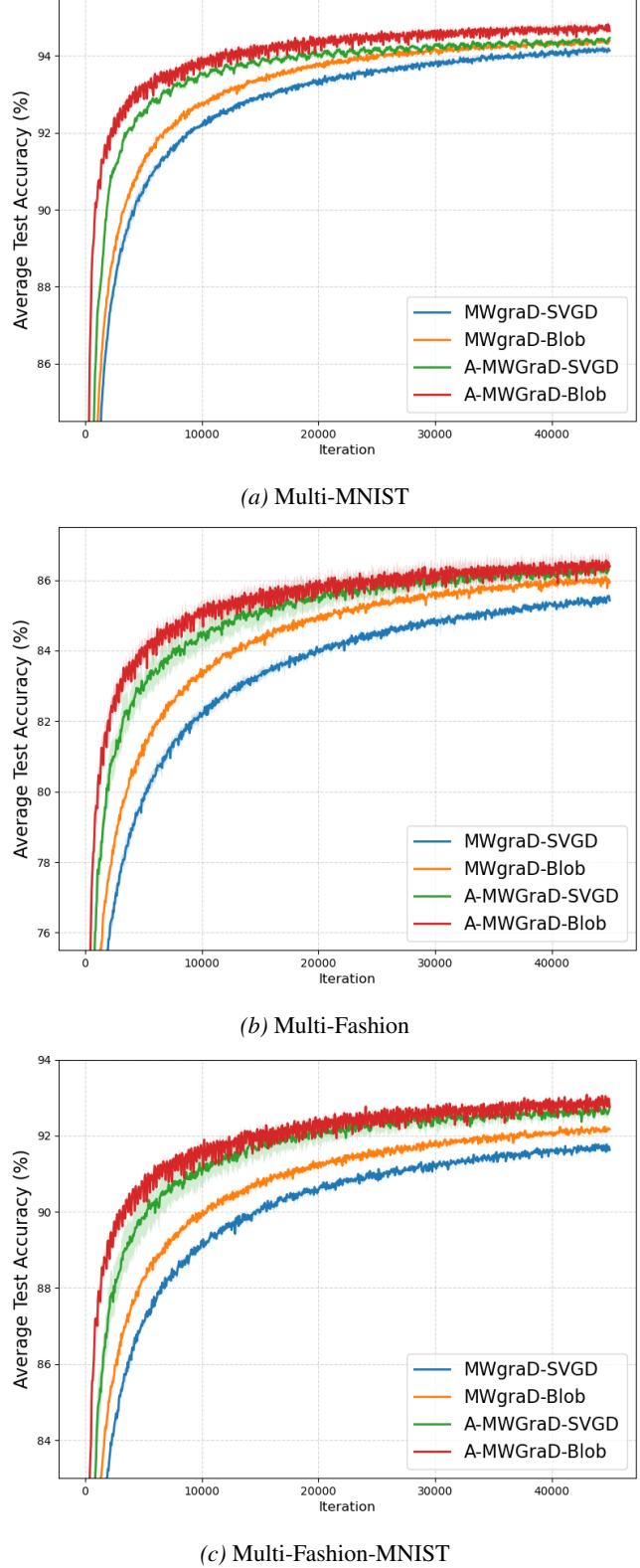


Figure 2. Evaluation of the average test accuracies over 40000 training iterations on datasets: (a) Multi-MNIST, (b) Multi-Fashion, and (c) Multi-Fashion-MNIST.

Datasets	Tasks	MOO-SVGD	MWGraD-SVGD	MWGraD-Blob	A-MWGraD-SVGD	A-MWGraD-Blob
Multi-Fashion +MNIST	#1	94.8±0.4	94.7±0.3	94.1±0.5	96.4±0.4	96.1±0.5
	#2	85.6±0.2	88.9±0.6	90.5±0.4	90.3±0.3	90.7±0.4
Multi-MNIST	#1	93.1±0.3	95.3±0.7	94.9±0.2	95.3±0.5	95.6±0.4
	#2	91.2±0.2	92.9±0.5	93.6±0.5	93.4±0.4	94.2±0.4
Multi-Fashion	#1	83.8±0.8	85.9±0.6	85.8±0.3	85.1±0.4	86.3±0.5
	#2	83.1±0.3	85.6±0.5	86.3±0.5	87.4±0.6	86.5±0.7

Table 1. Experimental results on Multi-Fashion+MNIST, Multi-MNIST, and Multi-Fashion. Ensemble accuracy (higher is better) averaged over three independent runs with different initializations.

4.2. Experiments on Bayesian multi-task learning

We follow the experimental setup described in (Phan et al., 2022; Nguyen et al., 2025) to evaluate the acceleration effect of A-MWGraD on real-world datasets.

Bayesian Multi-task Learning. We consider K prediction tasks with a training dataset \mathbb{D} . For each task $k \in [K]$, the model parameters are $\theta^k = [\mathbf{x}, \mathbf{z}^k]$, where \mathbf{x} denotes the shared component and \mathbf{z}^k denotes the task-specific, non-shared component. Following (Phan et al., 2022), we maintain a set of m models $\theta_i = [\theta_i^k]_{k=1}^K$, where $i \in [m]$, and $\theta_i^k = [\mathbf{x}_i, \mathbf{z}_i^k]$. At each iteration, given the non-shared components \mathbf{z}_i^k for $i \in [m], k \in [K]$, we sample the shared component from the multiple target distributions $p(\mathbf{x}|\mathbf{z}^k, \mathbb{D})$, $k \in [K]$ using either MWGraD or A-MWGraD variants. Then, for each task k , we update the non-shared components $[\mathbf{z}_i^k]_{i=1}^m$ by sampling from the posterior $p(\mathbf{z}^k|\mathbf{x}, \mathbb{D})$. This procedure corresponds to conventional Bayesian sampling, which can be implemented using SVGD or Blob methods, or a neural network (Nguyen et al., 2025; Phan et al., 2022). In our experiments, we use SVGD to sample the non-shared components and compare different methods for the shared component, including MOO-SVGD, MT-SGD, MWGraD variants (MWGraD-SVGD and MWGraD-Blob), our proposed A-MWGraD variants (A-MWGraD-SVGD and A-MWGraD-Blob).

Datasets and Evaluation Metric. We evaluate the methods on three benchmark datasets: Multi-Fashion-MNIST (Sabour et al., 2017), Multi-MNIST (Phan et al., 2022), and Multi-Fashion (Phan et al., 2022). Each dataset contains 120,000 training and 20,000 testing images, constructed by overlaying images from MNIST and FashionMNIST. This results in a two-task prediction setting, where each input image has two labels. We compare our methods against MOO-SVGD, MT-SGD and MWGraD variants, which achieved the state-of-the-art performance (Phan et al., 2022; Nguyen et al., 2025). For MT-SGD, MWGraD and A-MWGraD, results are reported from the ensemble prediction of five particle models. For MGDA, we train five independently initialized particle models. We evaluate the performance of the compared methods using task-wise

accuracies and the average accuracy across two tasks.

Results. Following the toy example, we evaluate the acceleration effect of A-MWGraD by comparing MWGraD variants (MWGraD-SVGD and MWGraD-Blob) with their accelerated counterparts (A-MWGraD-SVGD and A-MWGraD-Blob) in terms of the average test accuracy over training iterations. Figure 2 reports the mean accuracy (of two task-wise accuracies) averaged over five independent trials in 40000 iterations for the three considered datasets. We observe that, on most datasets, A-MWGraD variants reach higher test accuracy faster than MWGraD, demonstrating the acceleration effect of A-MWGraD for these tasks. Table 1 reports the test ensemble accuracy of compared methods for each task after 40000 iterations. We observe that variants of A-MWGraD consistently outperform other methods. For instance, A-MWGraD-SVGD and A-MWGraD-Blob achieve the best performance of 96.4% and 90.2% for task 1 and 2, respectively, on Multi-Fashion+MNIST. On Multi-MNIST, A-MWGraD-Blob achieves the best performance on both tasks (95.6% and 94.2%). These results show that A-MWGraD variants outperform MWGraD variants not only in convergence speed but also sampling effectiveness on multi-target sampling tasks.

5. Conclusions

We studied multi-objective optimization over probability spaces (MODO) and focused on the MWGraD algorithm (Nguyen et al., 2023), designed to solve this problem. We proposed A-MWGraD, an accelerated variant of MWGraD, based on damped Hamiltonian dynamics underlying Nesterov’s acceleration (Nesterov, 2013). We further conducted both theoretical and empirical analyses to demonstrate its acceleration effect relative to the original method. Despite these advances, several limitations remain: (i) the discrete-time convergence rates of A-MWGraD remain unestablished, and (ii) our convergence analysis assumes exact computation of Wasserstein gradients of all objectives, which is generally infeasible in practice. Our future work will address these issues and explore broader applications of MODO and A-MWGraD beyond multi-task learning.

Impact Statement

This paper presents work whose goal is to advance the field of Bayesian Machine Learning. There are many potential social consequences to collecting user data, even privately, none of which we feel must be specified here.

References

Attouch, H. and Garrigos, G. Multiobjective optimization: an inertial dynamical approach to pareto optima. *arXiv preprint arXiv:1506.02823*, 2015.

Carrillo, J. A., Craig, K., and Patacchini, F. S. A blob method for diffusion. *Calculus of Variations and Partial Differential Equations*, 58:1–53, 2019.

Liu, Q. and Wang, D. Stein variational gradient descent: A general purpose bayesian inference algorithm. *Advances in neural information processing systems*, 29, 2016.

Liu, X., Tong, X., and Liu, Q. Profiling pareto front with multi-objective stein variational gradient descent. *Advances in Neural Information Processing Systems*, 34: 14721–14733, 2021.

Maddison, C. J., Paulin, D., Teh, Y. W., O’Donoghue, B., and Doucet, A. Hamiltonian descent methods. *arXiv preprint arXiv:1809.05042*, 2018.

Nemirovskij, A. S. and Yudin, D. B. Problem complexity and method efficiency in optimization. 1983.

Nesterov, Y. Gradient methods for minimizing composite functions. *Mathematical programming*, 140(1):125–161, 2013.

Nguyen, D. H. and Sakurai, T. Mirror variational transport: a particle-based algorithm for distributional optimization on constrained domains. *Machine Learning*, 112(8):2845–2869, 2023.

Nguyen, D. H. and Sakurai, T. Moreau-yoshida variational transport: a general framework for solving regularized distributional optimization problems. *Machine Learning*, 113(9):6697–6724, 2024.

Nguyen, D. H. and Tsuda, K. On a linear fused gromov-wasserstein distance for graph structured data. *Pattern Recognition*, 138:109351, 2023.

Nguyen, D. H., Sakurai, T., and Mamitsuka, H. Wasserstein gradient flow over variational parameter space for variational inference. *arXiv preprint arXiv:2310.16705*, 2023.

Nguyen, D. H., Mamitsuka, H., and Nakamura, A. Multiple wasserstein gradient descent algorithm for multi-objective distributional optimization. *arXiv preprint arXiv:2505.18765*, 2025.

Phan, H., Tran, N., Le, T., Tran, T., Ho, N., and Phung, D. Stochastic multiple target sampling gradient descent. *Advances in neural information processing systems*, 35: 22643–22655, 2022.

Sabour, S., Frosst, N., and Hinton, G. E. Dynamic routing between capsules. *Advances in neural information processing systems*, 30, 2017.

Santambrogio, F. Optimal transport for applied mathematicians. 2015.

Sawaragi, Y., NAKAYAMA, H., and TANINO, T. *Theory of multiobjective optimization*, volume 176. Elsevier, 1985.

Shi, B., Du, S. S., Jordan, M. I., and Su, W. J. Understanding the acceleration phenomenon via high-resolution differential equations. *Mathematical Programming*, 195(1): 79–148, 2022.

Sonntag, K. and Peitz, S. Fast convergence of inertial multi-objective gradient-like systems with asymptotic vanishing damping. *SIAM Journal on Optimization*, 34(3):2259–2286, 2024.

Su, W., Boyd, S., and Candes, E. J. A differential equation for modeling nesterov’s accelerated gradient method: Theory and insights. *Journal of Machine Learning Research*, 17(153):1–43, 2016.

Taghvaei, A. and Mehta, P. Accelerated flow for probability distributions. In *International conference on machine learning*, pp. 6076–6085. PMLR, 2019.

Tanabe, H., Fukuda, E. H., and Yamashita, N. Convergence rates analysis of a multiobjective proximal gradient method. *Optimization Letters*, 17(2):333–350, 2023.

Wang, Y. and Li, W. Accelerated information gradient flow. *Journal of Scientific Computing*, 90(1):11, 2022.

A. Detailed Proof of Lemma 3.2

Proof. Recall that

$$E(\rho, q) = \min_{k \in [K]} \{F_k(\rho) - F_k(q)\}.$$

Then

$$\begin{aligned} \sup_{\mathbf{F}^* \in \mathbf{F}(P_w^* \cap \Omega_{\mathbf{F}}(\mathbf{F}(\rho_0)))} \inf_{q \in \mathbf{F}^{-1}(\mathbf{F}^*)} E(\rho, q) &= \sup_{\mathbf{F}^* \in \mathbf{F}(P_w^* \cap \Omega_{\mathbf{F}}(\mathbf{F}(\rho_0)))} \min_{k \in [K]} \{F_k(\rho) - F_k^*\} \\ &= \sup_{q \in P_w^* \cap \Omega_{\mathbf{F}}(\mathbf{F}(\rho_0))} \min_{k \in [K]} \{F_k(\rho) - F_k(q)\}. \end{aligned}$$

Since $\rho \in \Omega_{\mathbf{F}}(\mathbf{F}(\rho_0))$, we have $F_k(\rho) \leq F_k(\rho_0)$ for $k = 1, 2, \dots, K$. Hence,

$$\begin{aligned} \sup_{q \in P_w^* \cap \Omega_{\mathbf{F}}(\mathbf{F}(\rho_0))} \min_{k \in [K]} \{F_k(\rho) - F_k(q)\} &= \sup_{q \in \Omega_{\mathbf{F}}(\mathbf{F}(\rho_0))} \min_{k \in [K]} \{F_k(\rho) - F_k(q)\} \\ &= \sup_{q \in \mathcal{P}_2(\mathcal{X})} \min_{k \in [K]} \{F_k(\rho) - F_k(q)\}, \end{aligned}$$

which completes the proof. \square

B. Detailed Proof of Theorem 3.4

In this section, we provide the detailed proof of Theorem 3.4. We first recall the following auxiliary result from (Sonntag & Peitz, 2024).

Lemma B.1. *Let $\{h_k\}_{k=1}^K$ be continuously differentiable functions $h_k : \mathbb{R}_{\geq 0} \rightarrow \mathbb{R}$, and define $h(t) = \min_{k \in [K]} h_k(t)$. Then:*

(i) *h is differentiable for almost every $t \geq 0$.*

(ii) *for almost every $t \geq 0$, there exists $k \in [K]$ such that $h(t) = h_k(t)$ and $\dot{h}(t) = \dot{h}_k(t)$.*

Let $\{\rho_t\}_{t \geq 0}$ be the solution of the MWGraD flow (9), and let $q \in \mathcal{P}_2(\mathcal{X})$ be an arbitrary reference distribution (e.g., $q \in P_w^*$).

We have the following lemma.

Lemma B.2. *$E(\rho_t, q)$ is non-increasing along the MWGraD flow (9), i.e.,*

$$\dot{E}(\rho_t, q) \leq 0.$$

Proof. For each objective,

$$E_k(\rho_t, q) = F_k(\rho_t) - F_k(q).$$

Differentiating yields

$$\dot{E}_k(\rho_t, q) = \int \langle \nabla \Phi_t, \nabla \delta_\rho F_k[\rho_t] \rangle d\rho_t. \quad (20)$$

From the MWGraD flow (9) and the definition of the projection operator (10),

$$\Phi_t = -h^* = -\arg \min_{h \in \mathcal{C}(\rho_t)} \int \langle \nabla h, \nabla h \rangle d\rho_t = -\arg \min_{h \in \mathcal{C}(\rho_t)} \mathcal{H}(h), \quad (21)$$

where $\mathcal{H}(h) = \int \langle \nabla h, \nabla h \rangle d\rho_t$.

The functional $\mathcal{H}(h)$ is convex with respect to h , and its first variation is

$$\delta_h \mathcal{H}(h) = -\nabla \cdot (\rho_t \nabla h).$$

Optimality implies

$$\int \delta_h \mathcal{H}(h^*)(h - h^*) d\mathbf{x} \geq 0,$$

which is equivalent to

$$-\int \nabla \cdot (\rho_t \nabla h^*)(h - h^*) d\mathbf{x} = \int \langle \nabla h - \nabla h^*, \nabla h^* \rangle d\rho_t \geq 0.$$

Choosing $h = \delta_\rho F_k[\rho_t] \in \mathcal{C}(p_t)$ and using $h^* = -\Phi_t$ in (21) gives

$$\int \langle \nabla \Phi_t, \nabla \delta_\rho F_k[\rho_t] \rangle d\rho_t \leq - \int \|\nabla \Phi_t\|^2 d\rho_t. \quad (22)$$

Combining (20) and (22) and using Lemma B.1,

$$\dot{E}(\rho_t, q) \leq - \int \|\nabla \Phi_t\|^2 d\rho_t \leq 0,$$

which concludes the proof. \square

Now we are ready to provide the proof of Theorem 3.4.

Proof. Recall the definition of Lyapunov functional

$$\mathcal{V}(q, t) = \frac{1}{2} \mathcal{W}_2^2(\rho_t, q) = \frac{1}{2} \int \|T_t(\mathbf{x}) - \mathbf{x}\|^2 d\rho_t(\mathbf{x}),$$

where T_t is the optimal transport mapping from ρ_t to q .

Differentiating $\mathcal{V}(q, t)$ with respect to t gives

$$\dot{\mathcal{V}}(q, t) = \int \langle T_t(\mathbf{x}) - \mathbf{x}, \dot{T}_t(\mathbf{x}) \rangle d\rho_t(\mathbf{x}) + \int \langle \nabla \Phi_t(\mathbf{x}), [\nabla T_t - \mathbf{I}_d] (T_t(\mathbf{x}) - \mathbf{x}) \rangle d\rho_t(\mathbf{x}), \quad (23)$$

where $\mathbf{I}_d \in \mathbb{R}^{d \times d}$ denotes the identity matrix.

Using the identity from (Wang & Li, 2022), we obtain

$$\int \langle T_t(\mathbf{x}) - \mathbf{x}, \dot{T}_t(\mathbf{x}) \rangle d\rho_t(\mathbf{x}) + \int \langle \nabla \Phi_t(\mathbf{x}), \nabla T_t(\mathbf{x}) (T_t(\mathbf{x}) - \mathbf{x}) \rangle d\rho_t(\mathbf{x}) = 0. \quad (24)$$

Using (23) and (24) gives

$$\dot{\mathcal{V}}(q, t) = \int \langle \nabla \Phi_t(\mathbf{x}), \mathbf{x} - T_t(\mathbf{x}) \rangle d\rho_t(\mathbf{x}).$$

By geodesic convexity of each F_k ($k = 1, 2, \dots, K$), it follows that

$$F_k(\rho_t) - F_k(q) \leq \int \langle \nabla \delta_\rho F_k[\rho_t](\mathbf{x}), \mathbf{x} - T_t(\mathbf{x}) \rangle d\rho_t(\mathbf{x}). \quad (25)$$

Multiplying each inequality (25) by $w_k^{(t)}$ and summing over k yields

$$\sum_{k=1}^K w_k^{(t)} (F_k(\rho_t) - F_k(q)) \leq - \int \langle \nabla \Phi_t(\mathbf{x}), \mathbf{x} - T_t(\mathbf{x}) \rangle d\rho_t(\mathbf{x}) = -\dot{\mathcal{V}}(q, t).$$

Hence

$$E(\rho_t, q) = \min_{k \in [K]} \{F_k(\rho_t) - F_k(q)\} \leq -\dot{\mathcal{V}}(q, t). \quad (26)$$

Integrating (26) over $[0, t]$ gives

$$\int_0^t E(\rho_s, q) ds \leq -(\mathcal{V}(q, t) - \mathcal{V}(q, 0)) \leq \mathcal{V}(q, 0),$$

where we used the fact that $\mathcal{V}(q, t) \geq 0$.

By Lemma B.2, $E(\rho_t, q)$ is non-increasing, so we have

$$E(\rho_t, q) \leq \frac{\mathcal{V}(q, 0)}{t} = \frac{1}{2t} \mathcal{W}_2^2(\rho_0, q).$$

By Assumption 3.1, we further obtain

$$\sup_{\mathbf{F}^* \in \mathbf{F}(P_w^* \cap \Omega_{\mathbf{F}}(\mathbf{F}(p_0)))} \inf_{q \in \mathbf{F}^{-1}(\{\mathbf{F}^*\})} E(\rho_t, q) \leq \frac{R}{2t}.$$

Finally, from Lemma B.2, $E_k(\rho_t, q) = F_k(\rho_t) - F_k(q)$ is non-increasing, which means that $F_k(\rho_t) \leq F_k(\rho_0)$ for $k = 1, 2, \dots, K$. Thus $\rho_t \in \Omega_{\mathbf{F}}(\mathbf{F}(p_0))$. Applying Lemma 3.2 gives

$$\mathcal{M}(\rho_t) = \sup_{q \in \mathcal{P}_2(\mathcal{X})} E(\rho_t, q) \leq \frac{R}{2t}.$$

□

C. Detailed Proof of Theorem 3.5

In this section, we present the detailed proof of Theorem 3.5.

Let $\{\rho_t\}_{t \geq 0}$ be a solution of the A-MWGrad flow (13). For each $k \in [K]$, define the following global energy

$$W_k(t) = F_k(\rho_t) + \frac{1}{2} \int \|\nabla \Phi_t\|^2 d\rho_t.$$

We have the following lemma.

Lemma C.1. *For all $k \in [K]$, it follows that*

$$\dot{W}_k(t) \leq -\alpha_t \int \|\nabla \Phi_t\|^2 d\rho_t \leq 0.$$

Proof. Differentiating $W_k(t)$ with respect to t gives

$$\begin{aligned} \dot{W}_k(t) &= \dot{F}_k(\rho_t) + \frac{1}{2} \int \partial_t \|\nabla \Phi_t\|^2 d\rho_t + \frac{1}{2} \int \|\nabla \Phi_t\|^2 \dot{\rho}_t d\mathbf{x} \\ &= \int \langle \nabla \Phi_t, \nabla \delta_\rho F_k[\rho_t] \rangle d\rho_t + \int \langle \nabla \Phi_t, \partial_t \nabla \Phi_t \rangle d\rho_t + \int \langle \nabla \Phi_t, \frac{1}{2} \nabla \|\nabla \Phi_t\|^2 \rangle d\rho_t \\ &= \int \langle \nabla \Phi_t, \nabla \delta_\rho F_k[\rho_t] + \partial_t \nabla \Phi_t + \frac{1}{2} \nabla \|\nabla \Phi_t\|^2 \rangle d\rho_t, \end{aligned}$$

where we used the following identity $\dot{\rho}_t = -\nabla \cdot (\rho_t \nabla \Phi_t)$ and applied integration by parts.

Definition of A-MWGrad flow (13) gives

$$\begin{aligned} -\alpha_t \Phi_t &= \dot{\Phi}_t + \frac{1}{2} \|\nabla \Phi_t\|^2 + \text{prox}_{\mathcal{C}(\rho_t), \rho_t}[0] = \text{prox}_{\mathcal{C}(\rho_t) + \dot{\Phi}_t + \frac{1}{2} \|\nabla \Phi_t\|^2, \rho_t}[0] \\ &= \arg \min_{h \in \mathcal{C}(\rho_t) + \dot{\Phi}_t + \frac{1}{2} \|\nabla \Phi_t\|^2} \mathcal{G}(h), \end{aligned}$$

where $\mathcal{G}(h) = \int \langle \nabla h, \nabla h \rangle d\rho_t$ is the convex function with respect to h . Optimality gives

$$\int \delta_h G[h^*](h - h^*) d\mathbf{x} = \int \langle \nabla h^*, \nabla h - \nabla h^* \rangle d\rho_t \geq 0.$$

Choosing $h = \delta_\rho F_k[\rho_t] + \dot{\Phi}_t + \frac{1}{2} \|\nabla \Phi_t\|^2$ and using $h^* = -\alpha_t \Phi_t$, we have

$$\int \langle \nabla \Phi_t, \nabla \delta_\rho F_k[\rho_t] + \partial_t \nabla \Phi_t + \frac{1}{2} \nabla \|\nabla \Phi_t\|^2 \rangle d\rho_t \leq -\alpha_t \int \|\nabla \Phi_t\|^2 d\rho_t, \quad (27)$$

which concludes the proof. □

Due to the effect of damping term $-\alpha_t \Phi_t$, it is not guaranteed that $F_k(\rho_t)$ is non-increasing along the A-MWGrAD flow (13). However, the following corollary guarantees that $F_k(\rho_t)$ is upper bounded by the initial functional value $F_k(\rho_0)$ given $\nabla \Phi_0 = 0$.

Corollary C.2. *Let $\{\rho_t\}_{t \geq 0}$ be a solution of the A-MWGrAD flow (13) with $\nabla \Phi_0 = 0$. For $k \in [K]$, it holds that $F_k(\rho_t) \leq F_k(\rho_0)$, i.e., $\rho_t \in \Omega_F(\mathbf{F}(\rho_0))$, for all $t \geq 0$.*

Proof. From Lemma C.1, it follows that

$$F_k(\rho_0) = W_k(\rho_0) \geq F_k(\rho_t) + \frac{1}{2} \int \|\nabla \Phi_t\|^2 d\rho_t \geq F_k(\rho_t).$$

□

Now we are ready to present the proof of Theorem 3.5. We consider two cases for objectives F_k ($k \in [K]$): geodesically convex and β -strongly geodesically convex.

Consider F_k is geodesically convex for all $k \in [K]$ and define

$$\begin{aligned} \mathcal{E}_{k,\lambda}(\rho_t, q) &= t^2(F_k(\rho_t) - F_k(q)) + \frac{1}{2} \int \|2(\mathbf{x} - T_t(\mathbf{x})) + t\nabla \Phi_t(\mathbf{x})\|^2 d\rho_t(\mathbf{x}) \\ &\quad + \frac{\lambda}{2} \int \|\mathbf{x} - T_t(\mathbf{x})\|^2 d\rho_t(\mathbf{x}), \end{aligned}$$

and

$$\mathcal{E}(\rho_t, q) = \min_{k \in [K]} \mathcal{E}_{k,\lambda}(\rho_t, q).$$

We investigate the non-increasing of $\mathcal{E}_\lambda(\rho_t, q)$ through the following lemma.

Lemma C.3. *Suppose F_k is geodesically convex for $k \in [K]$. Let $\lambda = 2(\alpha - 3)$ and $\alpha \geq 3$. Then, it follows that*

$$\dot{\mathcal{E}}_{k,\lambda}(\rho_t, q) \leq 2t(F_k(\rho_t) - F_k(q)) - 2t \min_{l \in [K]} (F_l(\rho_t) - F_l(q)) + t(3 - \alpha) \int \|\nabla \Phi_t\|^2 d\rho_t. \quad (28)$$

Proof. Differentiating $\mathcal{E}_{k,\lambda}(t)$ with respect to t gives

$$\begin{aligned} \dot{\mathcal{E}}_{k,\lambda}(\rho_t, q) &= 2t(F_k(\rho_t) - F_k(q)) - t^2 \int \delta_\rho F_k[\rho_t] \nabla \cdot (\rho_t \nabla \Phi_t) d\mathbf{x} \\ &\quad + 4 \int \langle \partial_t T_t(\mathbf{x}), T_t(\mathbf{x}) - \mathbf{x} \rangle d\rho_t(\mathbf{x}) - 2 \int \|\mathbf{x} - T_t(\mathbf{x})\|^2 \nabla \cdot (\rho_t \nabla \Phi_t) d\mathbf{x} \\ &\quad + t \int \langle \nabla \Phi_t, \nabla \Phi_t + t \partial_t \nabla \Phi_t \rangle d\rho_t - \frac{1}{2} t^2 \int \|\nabla \Phi_t\|^2 \nabla \cdot (\rho_t \nabla \Phi_t) d\mathbf{x} \\ &\quad - 2 \int \langle \partial_t T_t, t \nabla \Phi_t \rangle d\rho_t + 2 \int \langle \mathbf{x} - T_t(\mathbf{x}), \nabla \Phi_t(\mathbf{x}) + t \partial_t \nabla \Phi_t(\mathbf{x}) \rangle d\rho_t(\mathbf{x}) \\ &\quad - 2t \int \langle \mathbf{x} - T_t(\mathbf{x}), \nabla \Phi_t(\mathbf{x}) \rangle \nabla \cdot (\rho_t \nabla \Phi_t) d\mathbf{x} \\ &\quad + \lambda \int \langle \partial_t T_t(\mathbf{x}), T_t(\mathbf{x}) - \mathbf{x} \rangle d\rho_t(\mathbf{x}) - \lambda \int \|\mathbf{x} - T_t(\mathbf{x})\|^2 \nabla \cdot (\rho_t \nabla \Phi_t) d\mathbf{x}. \end{aligned}$$

Here, we used the identity $\dot{\rho}_t = -\nabla \cdot (\rho_t \nabla \Phi_t)$.

By integration by parts, we obtain

$$\begin{aligned}
 \dot{\mathcal{E}}_{k,\lambda}(\rho_t, q) &= 2t(F_k(\rho_t) - F_k(q)) + t^2 \int \langle \nabla \Phi_t, \nabla \delta_\rho F_k[\rho_t] \rangle d\rho_t \\
 &+ 4 \int \langle \partial_t T_t(\mathbf{x}), T_t(\mathbf{x}) - \mathbf{x} \rangle d\rho_t(\mathbf{x}) + 4 \int \langle \nabla \Phi_t(\mathbf{x}), [\mathbf{I}_d - \nabla T_t(\mathbf{x})](\mathbf{x} - T_t(\mathbf{x})) \rangle d\rho_t(\mathbf{x}) \\
 &+ t \int \|\nabla \Phi_t\|^2 d\rho_t + t^2 \int \langle \nabla \Phi_t, \partial_t \nabla \Phi_t \rangle d\rho_t + t^2 \int \langle \nabla \Phi_t, \frac{1}{2} \nabla \|\nabla \Phi_t\|^2 \rangle d\rho_t \\
 &- 2t \int \langle \nabla \Phi_t, \partial_t T_t \rangle d\rho_t + 2 \int \langle \mathbf{x} - T_t(\mathbf{x}), \nabla \Phi_t(\mathbf{x}) + t \partial_t \nabla \Phi_t(\mathbf{x}) \rangle d\rho_t(\mathbf{x}) \\
 &+ 2t \int \langle \nabla \Phi_t(\mathbf{x}), [\mathbf{I}_d - \nabla T_t(\mathbf{x})] \nabla \Phi_t(\mathbf{x}) \rangle d\rho_t(\mathbf{x}) + 2t \int \langle \nabla \Phi_t(\mathbf{x}), [\nabla^2 \Phi_t(\mathbf{x})](\mathbf{x} - T_t(\mathbf{x})) \rangle d\rho_t(\mathbf{x}) \\
 &+ \lambda \int \langle \partial_t T_t(\mathbf{x}), T_t(\mathbf{x}) - \mathbf{x} \rangle d\rho_t(\mathbf{x}) + \lambda \int \langle \nabla \Phi_t(\mathbf{x}), [\mathbf{I}_d - \nabla T_t(\mathbf{x})](\mathbf{x} - T_t(\mathbf{x})) \rangle d\rho_t(\mathbf{x}).
 \end{aligned}$$

Rearranging the terms above gives

$$\begin{aligned}
 \dot{\mathcal{E}}_{k,\lambda}(\rho_t, q) &= 2t(F_k(\rho_t) - F_k(q)) + t^2 \int \langle \nabla \Phi_t, \nabla \delta_\rho F_k[\rho_t] + \frac{1}{2} \nabla \|\nabla \Phi_t\|^2 + \partial_t \nabla \Phi_t \rangle d\rho_t \\
 &+ t \int \langle T_t(\mathbf{x}) - \mathbf{x}, -\frac{6+\lambda}{t} \nabla \Phi_t - 2\partial_t \nabla \Phi_t - \nabla \|\nabla \Phi_t\|^2 \rangle d\rho_t(\mathbf{x}) \\
 &+ 3t \int \|\nabla \Phi_t\|^2 d\rho_t - 2t \int \langle \nabla \Phi_t, \nabla T_t \nabla \Phi_t \rangle d\rho_t - 2t \int \langle \nabla \Phi_t, \partial_t T_t \rangle d\rho_t \\
 &+ (4 + \lambda) \left(\int \langle \nabla \Phi_t(\mathbf{x}), [\nabla T_t(\mathbf{x})](T_t(\mathbf{x}) - \mathbf{x}) \rangle d\rho_t(\mathbf{x}) + \int \langle \partial_t T_t(\mathbf{x}), T_t(\mathbf{x}) - \mathbf{x} \rangle d\rho_t(\mathbf{x}) \right).
 \end{aligned} \tag{29}$$

Next, we have the following useful equality and inequality in (Wang & Li, 2022):

$$\int \langle \partial_t T_t, \nabla \Phi_t \rangle d\rho_t(\mathbf{x}) + \int \langle \nabla \Phi_t, \nabla T_t \nabla \Phi_t \rangle d\rho_t(\mathbf{x}) \geq 0, \tag{30}$$

$$\int \langle \partial_t T_t(\mathbf{x}), T_t(\mathbf{x}) - \mathbf{x} \rangle d\rho_t(\mathbf{x}) + \int \langle \nabla \Phi_t(\mathbf{x}), \nabla T_t(\mathbf{x})(T_t(\mathbf{x}) - \mathbf{x}) \rangle d\rho_t(\mathbf{x}) = 0. \tag{31}$$

By (30) and (31), we can simplify (29) as follows

$$\begin{aligned}
 \dot{\mathcal{E}}_{k,\lambda}(\rho_t, q) &= 2t(F_k(\rho_t) - F_k(q)) + t^2 \int \langle \nabla \Phi_t, \nabla \delta_\rho F_k[\rho_t] + \nabla \|\nabla \Phi_t\|^2 + \partial_t \nabla \Phi_t \rangle d\rho_t(\mathbf{x}) \\
 &+ t \int \langle T_t(\mathbf{x}) - \mathbf{x}, -\frac{6+\lambda}{t} \nabla \Phi_t - 2\partial_t \nabla \Phi_t - \nabla \|\nabla \Phi_t\|^2 \rangle d\rho_t(\mathbf{x}) \\
 &+ 3t \int \|\nabla \Phi_t\|^2 d\rho_t(\mathbf{x}).
 \end{aligned} \tag{32}$$

By definition of the A-MWGrad flow (13), we have

$$-\partial_t \nabla \Phi_t - \frac{\alpha}{t} \nabla \Phi_t - \frac{1}{2} \nabla \|\nabla \Phi_t\|^2 = \sum_{k=1}^K w_k^{(t)} \nabla \delta_\rho F_k[\rho_t]. \tag{33}$$

By using (27) of Lemma C.1, $\lambda = 2(\alpha - 3)$, and (33), we can upper bound (32) as follows

$$\begin{aligned}
 \dot{\mathcal{E}}_{k,\lambda}(\rho_t, q) &\leq 2t(F_k(p_t) - F_k(q)) - \alpha t \int \|\nabla \Phi_t\|^2 d\rho_t \\
 &\quad + 2t \int \langle T_t(\mathbf{x}) - \mathbf{x}, \sum_{k=1}^K w_k^{(t)} \nabla \delta_\rho F_k[\rho_t](\mathbf{x}) \rangle d\rho_t(\mathbf{x}) \\
 &\quad + 3t \int \|\nabla \Phi_t\|^2 d\rho_t \\
 &\leq 2t(F_k(p_t) - F_k(q)) - 2t \min_{l \in [K]} (F_l(p_t) - F_l(q)) + t(3 - \alpha) \int \|\nabla \Phi_t\|^2 d\rho_t,
 \end{aligned}$$

which conclude the proof of Lemma C.3. \square

Consider F_k is β -strongly geodesically convex for $k \in [K]$. Motivated by (Taghvaei & Mehta, 2019; Wang & Li, 2022), we define the following function

$$\mathcal{E}_k(\rho_t, q) = e^{\sqrt{\beta}t} (F_k(\rho_t) - F_k(q)) + \frac{e^{\sqrt{\beta}t}}{2} \int \|\sqrt{\beta}(\mathbf{x} - T_t(\mathbf{x})) + \nabla \Phi_t(\mathbf{x})\|^2 d\rho_t(\mathbf{x}),$$

and

$$\mathcal{E}(\rho_t, q) = \min_{k \in [K]} \mathcal{E}_k(\rho_t, q).$$

We investigate the non-increasing of $\mathcal{E}(\rho_t, q)$ through the following lemma.

Lemma C.4. Suppose F_k is β -strongly geodesically convex for $k \in [K]$. Let $\alpha_t = 2\sqrt{\beta}$. Then it follows that

$$e^{-\sqrt{\beta}t} \dot{\mathcal{E}}_k(\rho_t, q) \leq \sqrt{\beta} \mathcal{G}_k(\rho_t, q) - \sqrt{\beta} \min_{l \in [K]} \mathcal{G}_l(\rho_t, q) - \frac{\sqrt{\beta}}{2} \int \|\nabla \Phi_t\|^2 d\rho_t, \quad (34)$$

where $\mathcal{G}_k(\rho_t, q) = - \int \langle T_k(\mathbf{x}) - \mathbf{x}, \nabla \delta_\rho F_k[\rho_t](\mathbf{x}) \rangle d\rho_t(\mathbf{x})$.

Proof. Differentiating $\mathcal{E}_k(\rho_t, q)$ with respect to t gives

$$\begin{aligned}
 e^{-\sqrt{\beta}t} \dot{\mathcal{E}}_k(\rho_t, q) &= \sqrt{\beta} (F_k(\rho_t) - F_k(q)) - \int \delta_\rho F_k[\rho_t] \nabla \cdot (\rho_t \nabla \Phi_t) d\mathbf{x} \\
 &\quad + \frac{\sqrt{\beta^3}}{2} \int \|\mathbf{x} - T_t(\mathbf{x})\|^2 d\rho_t(\mathbf{x}) + \frac{\sqrt{\beta}}{2} \int \|\nabla \Phi_t\|^2 d\rho_t + \beta \int \langle \mathbf{x} - T_t(\mathbf{x}), \nabla \Phi_t(\mathbf{x}) \rangle d\rho_t(\mathbf{x}) \\
 &\quad + \beta \int \langle T_t(\mathbf{x}) - \mathbf{x}, \partial_t T_t(\mathbf{x}) \rangle d\rho_t(\mathbf{x}) - \frac{\beta}{2} \int \|\mathbf{x} - T_t(\mathbf{x})\|^2 \nabla \cdot (\rho_t \nabla \Phi_t) d\mathbf{x} \\
 &\quad + \int \langle \nabla \Phi_t(\mathbf{x}), \partial_t \nabla \Phi_t \rangle d\rho_t(\mathbf{x}) - \frac{1}{2} \int \|\nabla \Phi_t(\mathbf{x})\|^2 \nabla \cdot (\rho_t \nabla \Phi_t) d\mathbf{x} \\
 &\quad - \sqrt{\beta} \int \langle \partial_t T_t(\mathbf{x}), \nabla \Phi_t(\mathbf{x}) \rangle d\rho_t(\mathbf{x}) - \sqrt{\beta} \int \langle T_t(\mathbf{x}) - \mathbf{x}, \partial_t \Phi_t(\mathbf{x}) \rangle d\rho_t(\mathbf{x}) \\
 &\quad + \sqrt{\beta} \int \langle T_t(\mathbf{x}) - \mathbf{x}, \nabla \Phi_t(\mathbf{x}) \rangle \nabla \cdot (\rho_t \nabla \Phi_t) d\mathbf{x}
 \end{aligned} \quad (35)$$

By β -strongly geodesic convexity of F_k for $k \in [K]$, we obtain

$$\frac{\sqrt{\beta^3}}{2} \int \|\mathbf{x} - T_t(\mathbf{x})\|^2 d\rho_t(\mathbf{x}) + \sqrt{\beta} (F_k(\rho_t) - F_k(q)) \leq \sqrt{\beta} \int \langle T_t(\mathbf{x}) - \mathbf{x}, \nabla \delta_\rho F_k[\rho_t](\mathbf{x}) \rangle d\rho_t(\mathbf{x}) \quad (36)$$

Using the identity $\dot{\rho}_t = -\nabla \cdot (\rho_t \nabla \Phi_t)$ gives

$$\begin{aligned}
 & - \int \delta_\rho F_k[\rho_t] \nabla \cdot (\rho_t \nabla \Phi_t) d\mathbf{x} + \int \langle \nabla \Phi_t(\mathbf{x}), \partial_t \nabla \Phi_t(\mathbf{x}) \rangle d\rho_t(\mathbf{x}) \\
 & - \frac{1}{2} \int \|\nabla \Phi_t\|^2 \nabla \cdot (\rho_t \nabla \Phi_t) d\mathbf{x} \\
 & = \int \langle \Phi_t(\mathbf{x}), \nabla \delta_\rho F_k[\rho_t](\mathbf{x}) + \partial_t \nabla \Phi_t(\mathbf{x}) + \frac{1}{2} \nabla \|\nabla \Phi_t(\mathbf{x})\|^2 \rangle d\rho_t(\mathbf{x}) \\
 & \leq -\alpha_t \int \|\nabla \Phi_t(\mathbf{x})\|^2 d\rho_t(\mathbf{x}) = -2\sqrt{\beta} \int \|\nabla \Phi_t(\mathbf{x})\|^2 d\rho_t(\mathbf{x}),
 \end{aligned}$$

where we used (27) of the proof of Lemma C.1. We also have

$$\begin{aligned}
 & -\frac{\beta}{2} \int \|\mathbf{x} - T_t(\mathbf{x})\|^2 \nabla \cdot (\rho_t \nabla \Phi_t) d\mathbf{x} = \beta \int \langle \nabla \Phi_t(\mathbf{x}), [\nabla T_t(\mathbf{x}) - \mathbf{I}_d] (T_t(\mathbf{x}) - \mathbf{x}) \rangle d\rho_t(\mathbf{x}) \\
 & = \beta \int \langle \nabla \Phi_t(\mathbf{x}), [\nabla T_t(\mathbf{x})] (T_t(\mathbf{x}) - \mathbf{x}) \rangle d\rho_t(\mathbf{x}) - \beta \int \langle \nabla \Phi_t(\mathbf{x}), (T_t(\mathbf{x}) - \mathbf{x}) \rangle d\rho_t(\mathbf{x}).
 \end{aligned} \tag{37}$$

$$\begin{aligned}
 & \sqrt{\beta} \int \langle T_t(\mathbf{x}) - \mathbf{x}, \nabla \Phi_t(\mathbf{x}) \rangle \nabla \cdot (\rho_t \nabla \Phi_t) d\mathbf{x} = -\sqrt{\beta} \int \langle \nabla \Phi_t(\mathbf{x}), [\nabla T_t(\mathbf{x}) - \mathbf{I}] \nabla \Phi_t(\mathbf{x}) \rangle d\rho_t(\mathbf{x}) \\
 & - \sqrt{\beta} \int \langle \nabla \Phi_t(\mathbf{x}), \nabla^2 \Phi_t(\mathbf{x}) (T_t(\mathbf{x}) - \mathbf{x}) \rangle d\rho_t(\mathbf{x}) \\
 & = -\sqrt{\beta} \int \langle T_t(\mathbf{x}) - \mathbf{x}, \frac{1}{2} \nabla \|\nabla \Phi_t(\mathbf{x})\|^2 \rangle d\rho_t(\mathbf{x}) - \sqrt{\beta} \int \langle \nabla \Phi_t(\mathbf{x}), \nabla T_t(\mathbf{x}) \nabla \Phi_t(\mathbf{x}) \rangle d\rho_t(\mathbf{x}) \\
 & + \sqrt{\beta} \int \|\nabla \Phi_t(\mathbf{x})\|^2 d\rho_t(\mathbf{x})
 \end{aligned} \tag{38}$$

By (30), (31), (36), (37) and (38), we can simplify (35) as follows

$$\begin{aligned}
 e^{-\sqrt{\beta}t} \dot{\mathcal{E}}_k(\rho_t, q) & \leq -\sqrt{\beta} \int \langle T_t(\mathbf{x}) - \mathbf{x}, \nabla \delta_\rho F_k[\rho_t] \rangle d\rho_t(\mathbf{x}) - \frac{\sqrt{\beta}}{2} \int \|\nabla \Phi_t(\mathbf{x})\|^2 d\rho_t(\mathbf{x}) \\
 & + \underbrace{\beta \int \langle \partial_t T_t(\mathbf{x}), T_t(\mathbf{x}) - \mathbf{x} \rangle d\rho_t(\mathbf{x}) + \beta \int \langle \nabla \Phi_t(\mathbf{x}), \nabla T_t(\mathbf{x}) (T_t(\mathbf{x}) - \mathbf{x}) \rangle d\rho_t(\mathbf{x})}_{=0} \\
 & - \underbrace{(\int \langle \partial_t T_t, \nabla \Phi_t \rangle d\rho_t(\mathbf{x}) + \int \langle \nabla \Phi_t, \nabla T_t \nabla \Phi_t \rangle d\rho_t(\mathbf{x}))}_{\geq 0} \\
 & - \sqrt{\beta} \int \langle T_t(\mathbf{x}) - \mathbf{x}, \frac{1}{2} \nabla \|\nabla \Phi_t(\mathbf{x})\|^2 + 2\sqrt{\beta} \nabla \Phi_t(\mathbf{x}) + \partial_t \nabla \Phi_t(\mathbf{x}) \rangle d\rho_t(\mathbf{x}) \\
 & = -\sqrt{\beta} \int \langle T_t(\mathbf{x}) - \mathbf{x}, \nabla \delta_\rho F_k[\rho_t] \rangle d\rho_t(\mathbf{x}) - \sqrt{\beta} \int \langle T_t(\mathbf{x}) - \mathbf{x}, \sum_{l=1}^K w_l^{(t)} \nabla \delta_\rho F_l[\rho_t] \rangle d\rho_t(\mathbf{x}) \\
 & = \sqrt{\beta} \mathcal{G}_k(\rho_t, q) - \sqrt{\beta} \sum_{l=1}^K w_l^{(t)} \mathcal{G}_l(\rho_t, q) - \frac{\sqrt{\beta}}{2} \int \|\nabla \Phi_t(\mathbf{x})\|^2 d\rho_t(\mathbf{x}) \\
 & \leq \sqrt{\beta} \mathcal{G}_k(\rho_t, q) - \sqrt{\beta} \min_{l \in [K]} \mathcal{G}_l(\rho_t, q) - \frac{\sqrt{\beta}}{2} \int \|\nabla \Phi_t(\mathbf{x})\|^2 d\rho_t(\mathbf{x})
 \end{aligned} \tag{39}$$

which concludes the proof of Lemma C.4. \square

Now we are ready to present the proof of Theorem 3.5 using Lemma C.3 and Lemma C.4.

Proof. We first focus on proving (14) for the geodesically convex case. From Lemma B.1, we can see that for $t \geq 0$, then there exists k such that $\mathcal{E}_\lambda(\rho_t, q) = \mathcal{E}_{k,\lambda}(\rho_t, q)$ and $\dot{\mathcal{E}}_\lambda(t) = \dot{\mathcal{E}}_{k,\lambda}(t)$. Thus, by Lemma C.3, we obtain

$$\dot{\mathcal{E}}_\lambda(\rho_t, q) = \dot{\mathcal{E}}_{k,\lambda}(\rho_t, q) \leq 2t(F_k(\rho_t) - F_k(q)) - 2t(F_k(\rho_t) - F_k(q)) + t(3 - \alpha) \int \|\nabla \Phi_t\|^2 d\rho_t(\mathbf{x}).$$

Choosing $\alpha \geq 3$ gives: $\dot{\mathcal{E}}_\lambda(\rho_t, q) \leq 0$, which confirms its non-increasing. Thus, we obtain

$$\begin{aligned} t^2 \min_{k \in [K]} (F_k(\rho_t) - F_k(q)) &\leq \mathcal{E}_\lambda(\rho_t, q) \leq \mathcal{E}_\lambda(\rho_0, q) = (\alpha - 1) \int \|\mathbf{x} - T_t(\mathbf{x})\|^2 d\rho_t(\mathbf{x}) \\ &= (\alpha - 1) \mathcal{W}_2^2(\rho_0, q). \end{aligned}$$

We follow similar steps in proof of Theorem 3.4. By Assumption 3.1, we obtain

$$\sup_{\mathbf{F}^* \in \mathbf{F}(P_w^* \cap \Omega_{\mathbf{F}}(\mathbf{F}(p_0)))} \inf_{q \in \mathbf{F}^{-1}(\{\mathbf{F}^*\})} \min_{k \in [K]} (F_k(p_t) - F_k(q)) \leq \frac{(\alpha - 1)R}{t^2}.$$

We get:

$$\sup_{\mathbf{F}^* \in \mathbf{F}(P_w^* \cap \Omega_{\mathbf{F}}(\mathbf{F}(p_0)))} \min_{k \in [K]} \{F_k(p_t) - F_k^*\} \leq \frac{(\alpha - 1)R}{t^2},$$

which gives:

$$\sup_{q \in P_w^* \cap \Omega_{\mathbf{F}}(\mathbf{F}(p_0))} \min_{k \in [K]} \{F_k(p_t) - F_k(q)\} \leq \frac{(\alpha - 1)R}{t^2}.$$

Furthermore, as shown in Corollary C.2, $F_k(\rho_t) \leq F_k(\rho_0)$ for all k , which ensures that $\rho_t \in \Omega_{\mathbf{F}}(\mathbf{F}(p_0))$. Applying Lemma 3.2, we conclude the proof of (14).

Next we focus on proving (15) for the β -strongly geodesically convex case. Simiarly, from Lemma B.1, we have that for $t \geq 0$, there exists k such that $\mathcal{E}(\rho_t, q) = \mathcal{E}_k(\rho_t, q)$ and $\dot{\mathcal{E}}(\rho_t, q) = \dot{\mathcal{E}}_k(\rho_t, q)$. Thus, by Lemma C.4, we get:

$$e^{-\sqrt{\beta}t} \dot{\mathcal{E}}(\rho_t, q) = e^{-\sqrt{\beta}t} \min_{l \in [K]} \dot{\mathcal{E}}_l(\rho_t, q) \leq -\frac{\sqrt{\beta}}{2} \int \|\nabla \Phi_t(\mathbf{x})\|^2 d\rho_t(\mathbf{x}) \leq 0.$$

This gives: $\dot{\mathcal{E}}(\rho_t, q) \leq 0$, which confirms its non-increasing. Thus, we obtain

$$\min_{k \in [K]} \{F_k(\rho_t) - F_k(q)\} \leq e^{-\sqrt{\beta}t} \left[\min_{l \in [K]} \{F_l(\rho_0) - F_l(q)\} + \frac{\beta}{2} \mathcal{W}_2^2(\rho_0, q) \right].$$

Here we remark that for any $q \in P_w^* \cap \Omega_{\mathbf{F}}(\mathbf{F}(p_0))$, we get $\min_{l \in [K]} \{F_l(\rho_0) - F_l(q)\} \leq \min_{l \in [K]} F_l(\rho_0)$ and $\mathcal{W}_2^2(\rho_0, q) \leq R$. Hence,

$$\sup_{\mathbf{F}^* \in \mathbf{F}(P_w^* \cap \Omega_{\mathbf{F}}(\mathbf{F}(p_0)))} \inf_{q \in \mathbf{F}^{-1}(\{\mathbf{F}^*\})} \min_{k \in [K]} (F_k(p_t) - F_k(q)) \leq e^{-\sqrt{\beta}t} \left[\min_{l \in [K]} F_l(\rho_0) + \frac{\beta R}{2} \right].$$

Finally, applying Lemma 3.2, we concludes the proof of (15). □

D. Detailed Derivation of (16)

Starting from (13), we have

$$\dot{\rho}_t + \nabla \cdot (\rho_t \nabla \Phi_t) = 0,$$

which is the continuity equation of ρ_t . At the particle level, each particle \mathbf{x}_t evolves according to

$$\dot{\mathbf{x}}_t = \nabla \Phi_t(\mathbf{x}_t).$$

Let define the velocity $\mathbf{v}_t = \nabla \Phi_t(\mathbf{x}_t)$, its time derivative is

$$\begin{aligned}\dot{\mathbf{v}}_t &= \partial_t \nabla \Phi_t(\mathbf{x}_t) + [\nabla^2 \Phi_t(\mathbf{x}_t)] \nabla \Phi_t(\mathbf{x}_t) \\ &= \left(-\alpha_t \nabla \Phi_t(\mathbf{x}_t) - [\nabla^2 \Phi_t(\mathbf{x}_t)] \nabla \Phi_t(\mathbf{x}_t) - \sum_{k=1}^K w_k^{(t)} \nabla \delta_\rho F_k[\rho_t](\mathbf{x}_t) \right) + [\nabla^2 \Phi_t(\mathbf{x}_t)] \nabla \Phi_t(\mathbf{x}_t) \\ &= -\alpha_t \mathbf{v}_t - \sum_{k=1}^K w_k^{(t)} \nabla \delta_\rho F_k[\rho_t](\mathbf{x}_t).\end{aligned}$$

This gives the particle-level evolution equation (16) as desired.

E. Algorithms: MWGraD and A-MWGraD

Algorithm 1 Multi-objective Wasserstein Gradient Descent (MWGraD) (Nguyen et al., 2025)

Input: Functionals $\{F_k\}_{k=1}^K$, number of particles m , number of iterations T , step sizes $\eta > 0$.

Output: a set of m particles $\{\mathbf{x}_i^{(T)}\}_{i=1}^m$.

Sample m initial particles $\{\mathbf{x}_i^{(0)}\}_{i=1}^m$ from $\mathcal{N}(0, \mathbf{I}_d)$.

$n \leftarrow 0$

while $n < T$ **do**

 Estimate $\bar{\Delta}_k^{(n)}(\mathbf{x}_i^{(n)})$ by (17) or (18), for $i \in [m], k \in [K]$

 Compute $\mathbf{w}^{(n)}$ by solving (8)

 Update $\mathbf{x}_i^{(n+1)} \leftarrow \mathbf{x}_i^{(n)} - \eta \sum_{k=1}^K w_k^{(n)} \bar{\Delta}_k^{(n)}(\mathbf{x}_i^{(n)})$, for $i \in [m]$

$n \leftarrow n + 1$

end

Algorithm 2 Accelerated Multi-objective Wasserstein Gradient Descent (A-MWGraD) (This work)

Input: Functionals $\{F_k\}_{k=1}^K$, number of particles m , number of iterations T , step sizes $\eta > 0$.

Output: a set of m particles $\{\mathbf{x}_i^{(T)}\}_{i=1}^m$.

Sample m initial particles $\mathbf{x}_i^{(0)}$ from $\mathcal{N}(0, \mathbf{I}_d)$ and set initial velocities as $\mathbf{v}_i^{(0)} = 0$, for $i \in [m]$.

$n \leftarrow 0$

while $n < T$ **do**

 Estimate $\bar{\Delta}_k^{(n)}(\mathbf{x}_i^{(n)})$ by (17) or (18), for $i \in [m], k \in [K]$.

 Compute $\mathbf{w}^{(n)}$ by solving (8).

 Set $\alpha_n = \begin{cases} \frac{1-\sqrt{\beta\eta}}{1+\sqrt{\beta\eta}}, & \text{if all } F_k(k \in [K]) \text{ are } \beta\text{-strongly geodesically convex,} \\ \frac{n-1}{n+2}, & \text{if all } F_k(k \in [K]) \text{ are geodesically convex or } \beta \text{ is unknown.} \end{cases}$

 Update $\mathbf{x}_i^{(n+1)} \leftarrow \mathbf{x}_i^{(n)} + \sqrt{\eta} \mathbf{v}_i^{(n)}$.

 Update $\mathbf{v}_i^{(n+1)} \leftarrow \alpha_n \mathbf{v}_i^{(n)} - \sqrt{\eta} \sum_{k=1}^K w_k^{(n)} \bar{\Delta}_k^{(n)}(\mathbf{x}_i^{(n)})$, for $i \in [m]$.

$n \leftarrow n + 1$.

end

F. Additional Experimental Results

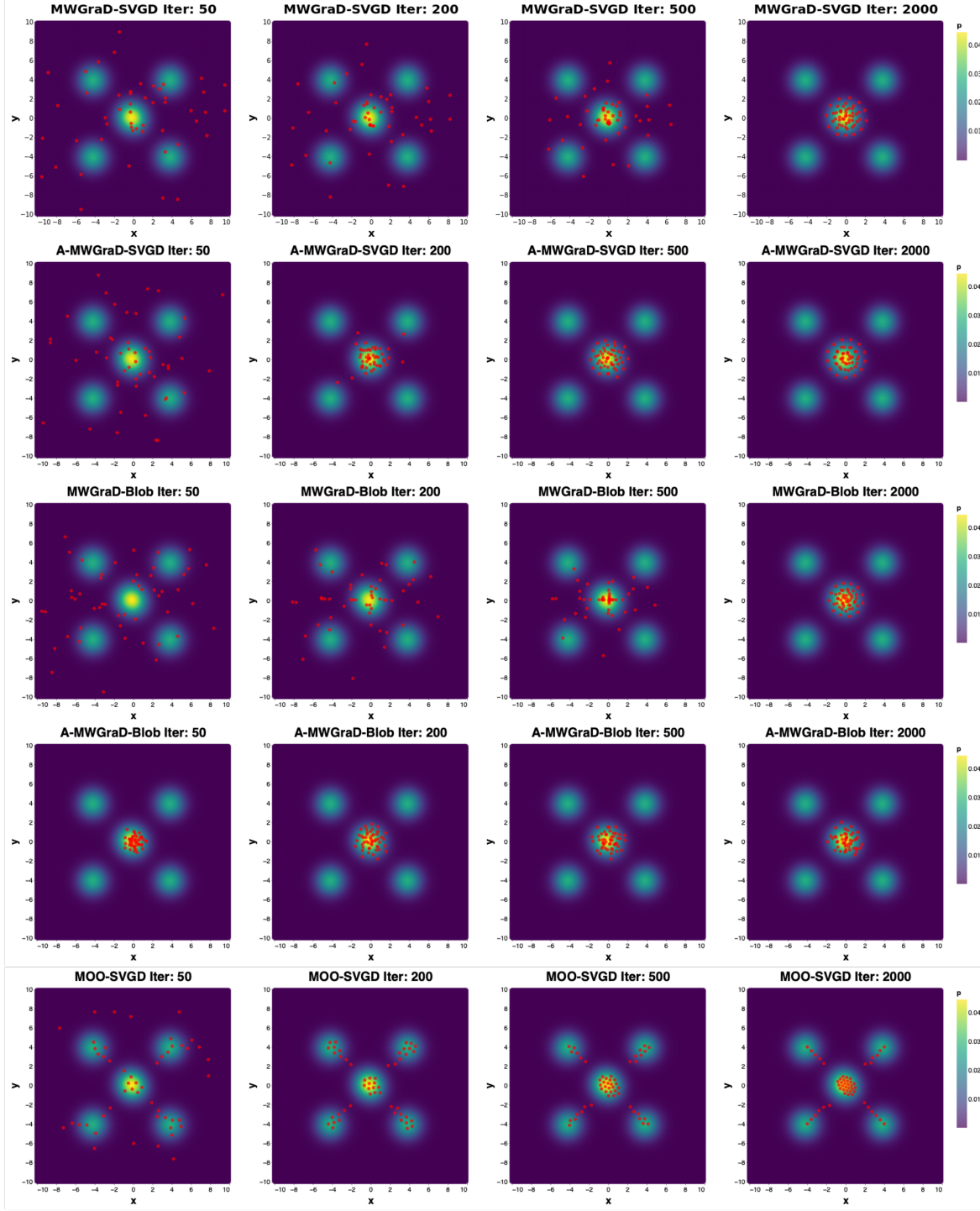


Figure 3. Sampling from multiple target distributions, where each target is a mixture of two Gaussians. These targets have a joint high-density region around the origin. Initially, 50 particles are sampled from the standard distribution, and then updated by MWGraD variants, A-MWGraD variants, and MOO-SVGD. While MOO-SVGD tends to scatter particles across all the modes (see the last row), MWGraD and A-MWGraD variants tend to move particles towards the joint high-density region. Furthermore, A-MWGraD variants converge faster than MWGraD variants.